

**UNIVERSIDADE DE SÃO PAULO
ESCOLA DE ENGENHARIA DE SÃO CARLOS**

Gustavo Miranda Hebling

**A Sparse and Numerically Stable Implementation of a
Distribution System State Estimator**

São Carlos

2022

Gustavo Miranda Hebling

**A Sparse and Numerically Stable Implementation of a
Distribution System State Estimator**

Dissertation presented to the São Carlos
School of Engineering of the University of
São Paulo, to obtain the degree of Master of
Science - Electrical Engineering.

Concentration Area: Electric Power Systems

Supervisor: Prof. Dr. João Bosco Augusto
London Junior

São Carlos

2022

Trata-se da versão corrigida da dissertação. A versão original se encontra disponível na EESC/USP que aloja o Programa de Pós-Graduação de Engenharia Elétrica.

AUTORIZO A REPRODUÇÃO TOTAL OU PARCIAL DESTE TRABALHO,
POR QUALQUER MEIO CONVENCIONAL OU ELETRÔNICO, PARA FINS
DE ESTUDO E PESQUISA, DESDE QUE CITADA A FONTE.

Ficha catalográfica elaborada pela Biblioteca Prof. Dr. Sérgio Rodrigues Fontes da
EESC/USP com os dados inseridos pelo(a) autor(a).

H443a Hebling, Gustavo Miranda
A Sparse and Numerically Stable Implementation of a
Distribution System State Estimator / Gustavo Miranda
Hebling; orientador João Bosco Augusto London Junior.
São Carlos, 2022.

Dissertação (Mestrado) - Programa de
Pós-Graduação em Engenharia Elétrica e Área de
Concentração em Sistemas Elétricos de Potência --
Escola de Engenharia de São Carlos da Universidade de
São Paulo, 2022.

1. Sistemas de Distribuição. 2. Estimação de
Estados. 3. Métodos Numéricos. 4. Esparsidade. 5.
Métodos Ortogonais. I. Título.

FOLHA DE JULGAMENTO

Candidato: Engenheiro **GUSTAVO MIRANDA HEBLING**.

Título da dissertação: "Uma implementação esparsa e numericamente estável de um estimulador de estado para sistemas de distribuição".

Data da defesa: 24/03/2022.

Comissão Julgadora

Resultado

Prof. Associado **João Bosco Augusto London Junior**
(Orientador)
(Escola de Engenharia de São Carlos – EESC/USP)

Aprovado

Profa. Dra. **Elizete Maria Lourenço**
(Universidade Federal do Paraná/UFPR)

Aprovado

Prof. Dr. **André Abel Augusto**
(Universidade Federal Fluminense/UFF)

Aprovado

Coordenador do Programa de Pós-Graduação em Engenharia Elétrica:
Prof. Associado **João Bosco Augusto London Junior**

Presidente da Comissão de Pós-Graduação:
Prof. Titular **Murilo Araujo Romero**

ACKNOWLEDGEMENTS

A lot of people, directly or indirectly, have contributed to this work, here are some acknowledgements:

To my parents, for their continuous support to my studies and encouragement to my career as an engineer. Thanks to them, I have a great interest and curiosity for science.

To Professor João Bosco, who was responsible for the beginning of my research career in 2015. In a moment of uncertainty, his advice cleared a path to electrical engineering and electric power systems. I am extremely thankful for the support and attention over all these years which were essential for my studies and this work.

To my friend and co-worker Julio Massignan. This work is a direct result of our partnership. As a friend, our conversations will be remembered.

This work is also dedicated to all the friends at LACOSEP, the teachers and workers from the Department of Electrical Engineering and the São Carlos School of Engineering.

“Somewhere, something incredible is waiting to be known.”
Carl Sagan

RESUMO

HEBLING, G. M. **Uma Implementação Esparsa e Numericamente Estável de um Estimador de Estado para Sistemas de Distribuição**. 2022. 73p. Dissertação (Mestrado) - Escola de Engenharia de São Carlos, Universidade de São Paulo, São Carlos, 2022.

O Estimador de Estado é a principal ferramenta para operação em tempo real de sistemas de potência. O estimador tem como principal função obter a condição operacional da rede dado um conjunto de medidas e seu processamento é o primeiro passo de uma série de ferramentas automáticas que fazem parte dos sistemas de gerenciamento da energia. Algoritmos especializados foram desenvolvidos para a estimação de estado em sistemas de distribuição uma vez que o Estimador de Mínimos Quadrados Ponderados (MQP), comumente usado em sistemas de transmissão, enfrenta dificuldades para o uso devido a características específicas de Sistemas de Distribuição (SDs). O Estimador MQP requer a solução de um sistema linear que pode ser mal condicionado em função de particularidades dos SDs como ramos mono, bi e trifásicos desbalanceados, grande número de barras e conexões entre linhas curtas e longas, entre outros.

A matriz Ganho, matriz de coeficientes do sistema linear obtido com o estimador MQP, é fatorada e a técnica usual chamada fatoração Cholesky pode criar elementos não-nulos induzindo ainda mais perturbações num sistema potencialmente mal condicionado, diminuindo a qualidade da solução. Dada a característica esparsa da matriz Ganho, técnicas específicas podem ser utilizadas para obter melhor performance computacional.

Nesse contexto, esse trabalho propõe uma formulação ortogonal do estimador MQP que visa melhorar a acuracidade da solução bem como a estabilidade numérica do processo de estimação. A fatoração QR é utilizada para obter uma matriz triangular superior que leva a substituições para solucionar o sistema linear. Técnicas dedicadas a matrizes esparsas são usadas para preservar essa característica e melhorar o tempo computacional do estimador.

Esse trabalho apresenta as bases teóricas da estimação de estado, as técnicas dedicadas a matrizes esparsas que permitem melhorar o desempenho computacional e a formulação ortogonal que melhora a estabilidade numérica da estimação. Os resultados compilam métricas de performance e acuracidade da proposta e comparações desta com algoritmos dedicados para SDs e também formulações alternativas do MQP.

Palavras-chave: Sistemas de Distribuição, Estimação de Estados, Métodos Numéricos, Esparsidade, Métodos Ortogonais.

ABSTRACT

HEBLING, G. M. **A Sparse and Numerically Stable Implementation of a Distribution System State Estimator**. 2022. 73p. Dissertation (Master) - Escola de Engenharia de São Carlos, Universidade de São Paulo, São Carlos, 2022.

The state estimator is the main analysis tool in real-time operation of power systems. It obtains the operating condition of the network given a set of measurements and this is the first step in a series of automated applications in energy management systems. Specialized algorithms have been developed to perform Distribution System State Estimation (DSSE) since the Weighted Least Squares (WLS) estimator, commonly used in transmission systems, faces challenges due to specific characteristics of Distribution Systems (DSs). The WLS estimator requires the solution of a linear system which may be ill-conditioned due to a set of particularities of DSs such as the one, two and three-phase unbalanced branches, large number of nodes and connections between long and short lines, among others.

The Gain matrix, the coefficient matrix of the linear system obtained with the WLS estimator, requires factoring and the usual technique, the Cholesky factorization, may create a large number of non-zero elements adding perturbations to an already ill-conditioned system which may impact the solution obtained. Since the Gain matrix is sparse, specialized techniques may be used to extract peak computational performance.

In this context, this work evaluates the use of an orthogonal formulation of the WLS state estimator which aims to improve the accuracy of the solution as well as the numerical stability of the estimation process. The QR factorization obtains an upper triangular linear system that can be solved with simple substitutions. Dedicated techniques are used to preserve the sparse structure of the matrices and with a sparse-oriented algorithm to obtain the QR factorization, the state estimation is executed in a very short running time, even for large test systems.

This work presents the theoretical background of state estimation, an overview of the sparse techniques that allow for higher computational performance and the orthogonal formulation which improves the numerical stability of the state estimation. Results are presented with performance and accuracy metrics for the proposed estimator and comparisons with a dedicated algorithm for DSs and alternative formulations of the WLS estimator.

Keywords: Distribution Systems, State Estimation, Numerical Methods. Sparsity, Orthogonal Methods.

LIST OF FIGURES

Figure 1 – Three-phase branch circuits. The impedance and capacitancy self parameters ($Z_{aa}, B_{aa}, Z_{bb}, B_{bb}, Z_{cc}, B_{cc}$) as well as mutual parameters ($Z_{ab}, B_{ab}, Z_{bc}, B_{bc}, Z_{ca}, B_{ca}$) are given by specific characteristic of the cables. Source: Author	30
Figure 2 – Three-phase transformer connections of the primary and secondary windings. Source: Author.	31
Figure 3 – Node elimination resulting in fill-ins. Source: Author	47
Figure 4 – Steps performed on the Multifrontal QR. Source: Author	48
Figure 5 – A sparse matrix, its factor R and the elimination tree obtained with the Multifrontal QR. Source: (DAVIS, 2015)	50
Figure 6 – Steps performed to obtain the estimated state with the orthogonal formulation of the state estimator.	53
Figure 7 – Topology of the 342 nodes system	56
Figure 8 – Sparse pattern of the matrices of the 342 nodes IEEE test system and its corresponding factors	57
Figure 9 – Sparsity pattern of the matrices of the 123 nodes IEEE test system	57
Figure 10 – Sparsity pattern of the ordered Gain matrix and its corresponding L factor, 342 nodes test system.	58
Figure 11 – Sparsity pattern of the ordered orthogonal QR matrix and its corresponding L factor, 342 nodes test system.	58
Figure 12 – Average MAE metric for all state variables	62
Figure 13 – KEMA metric for each Monte Carlo repetition	62

LIST OF TABLES

Table 1 – Submatrices of the two-port model based on the different connection type of the windings	31
Table 2 – Measurements sets for the three different test systems	55
Table 3 – Relative fill-in reduction with the Gain Matrix formulation	59
Table 4 – Relative fill-in reduction with the proposed QR formulation	59
Table 5 – Performance metrics obtained with the proposed estimator for each simulation scenario with the 342 nodes test system.	61
Table 6 – Detailed errors for all simulation scenarios obtained with the proposed estimator using the 342 nodes test system.	61
Table 7 – Condition number of the coefficient matrix for different estimators. . . .	63
Table 8 – Condition number of the coefficient matrix of the NEC estimator for different scaling factors.	63
Table 9 – Number of iterations necessary for convergence for each estimator without reordering the coefficient matrix.	64
Table 10 – Number of iterations necessary for convergence for each estimator using the AMD ordering method.	64
Table 11 – Number of iterations necessary for convergence for each estimator using the Nested Dissection ordering method.	65
Table 12 – Time necessary for convergence for each estimator without reordering the coefficient matrix.	65
Table 13 – Time necessary for convergence for each estimator using the AMD ordering method.	65
Table 14 – Time necessary for convergence for each estimator using the Nested Dissection ordering method.	66
Table 15 – Maximum MAE considering all Monte Carlo simulations.	66

CONTENTS

1	INTRODUCTION	19
1.1	Context	19
1.2	Objectives	21
1.3	Work Structure	22
2	DISTRIBUTION SYSTEMS STATE ESTIMATION	25
2.1	WLS State Estimator	25
2.2	Three Phase Models	27
2.2.1	Power lines and Transformers	29
2.2.2	Transformers	30
2.3	Measurement Types	32
2.4	Alternative WLS formulations	33
2.4.1	WLS with Equality Constraints	33
2.4.2	Hatchel Augmented Matrix Method	34
2.5	Dedicated Distribution System State Estimators	35
2.5.1	Branch-Current State Estimator	36
2.5.2	Admittance Matrix Based State Estimator	37
2.6	Summary	38
3	THE PROPOSED ORTHOGONAL WLS STATE ESTIMATOR	41
3.1	Motivation	41
3.2	Sparse Linear Systems	42
3.2.1	Theoretical Background	42
3.2.2	Linear System Solvers	43
3.2.3	Ordering Methods	46
3.2.4	Multifrontal QR	48
3.3	Proposed Formulation	50
4	RESULTS	55
4.1	Test Systems	55
4.2	Evaluation of Ordering Methods	56
4.3	Evaluation of the Proposed QR Estimator	59
4.4	Comparisons with Other Estimators	61
4.4.1	Numerical Aspects	62
4.4.2	Computational Aspects	64
5	CONCLUSIONS	67

5.1	Future Research	68
5.2	List of Publications	68
	REFERENCES	71

1 INTRODUCTION

1.1 Context

The power grid is an interconnected system whose main function is to deliver electrical energy generated via different sources to a wide range of consumers. The transmission system is responsible for transporting the energy from the generators, which can be coupled to different energy sources such as hydro, thermal, solar or wind, to populated areas where the consumers are located. The distribution system makes the interface between consumers and the transmission systems. Therefore, a safe, reliable and continuous power grid operation is required. These complex systems require monitoring tools to ensure a safe and reliable operation and the State Estimator is the main tool used to obtain the real-time condition of the network given a set of measurements originated from meters located on the grid (ABUR; EXPÓSITO, 2004; PRIMADIANTO; LU, 2017).

Historically, the application of State Estimation in Distribution Systems (DSs) was hindered because the total number of available real time measurements was lower than what is normally available for transmission systems. Therefore, the operational condition of distribution systems was inferred using load estimates based on each type of consumer: industrial, commercial or residential, and the quality of the inferred operational condition was dependent on the quality of the load profiles used to represent the feeders. More recently, however, the operating environment has been changing due to the penetration of renewable energy sources, energy storage, electric vehicles, and demand response. Given this scenario, the utilities face new challenges in real-time operation because of the large amount of data generated from new sensors, such as *smart meters*. In this context, accuracy and computational efficiency become two requirements of Distribution System State Estimation (DSSE) in order to obtain a reliable estimate of the network operational condition.

The state estimator is the first step to perform a wide range of automated applications in energy management systems, such as power flow, contingency analysis, load forecasting, stability margin calculations, short-circuit calculations and others. Since many of these applications provide the situational awareness of the grid in real time, the research on a fast and reliable state estimator for DSs is desired even more so with the expected increase in data volume at DSs operation centers.

Despite the consolidated position of the Weighted Least Squares (WLS) state estimator for transmission systems, specialized algorithms have been developed to perform DSSE because there are limitations to the WLS approach due to particular characteristics of DS such as (SINGH; PAL; JABR, 2009; BARAN, 2012; LEFEBVRE; PRÉVOST; LENOIR, 2014; KANJU, 2016; AHMAD *et al.*, 2018a): 1) DSs are usually operated at a

radial structure, that is, with one path from the substations to the consumers; 2) There are one, two (residential loads) and three-phase branches (commercial and industrial loads); 3) Lines are usually short, and untransposed; 4) Lines are unbalanced since the loads cannot be distributed symmetrically in the feeders; 5) There can be a large number of nodes and branches, even for small cities, which result in large dimensions for the matrices associated with the estimator; 6) The status of switches and capacitor banks, as well as transformers taps are not directly monitored;

These specific characteristics of DSs result in severe ill-conditioning of the coefficient matrix obtained with the WLS estimator, called Gain Matrix which must be factorized to obtain the estimated state when using the conventional WLS estimator. Besides the characteristics previously cited, the ill-conditioning is also associated with connections between long and short lines (ATANACKOVIC; DABIC, 2013) and the presence, in large numbers, of pseudo measurements given the scarcity of real-time measurements (MONTICELLI; MURARI; WU, 1985). The specialized algorithms for DSSE are alternative formulations that try to deal with the previously shown characteristics of DSs. Some approaches use a formulation based on the admittance matrix of the system (ALMEIDA; OCHOA, 2017), others use current flowing in the branches as state variables instead of nodal voltages (PAU; PEGORARO; SULIS, 2013a). These approaches are fundamentally different than the WLS estimator that uses the Gain matrix to obtain an update to the estimated state, instead, they solve an approximate problem that may not correspond fully to the original one (FENG; YANG; PETERSON, 2012).

The aforementioned dedicated formulations for DSSE make transformations on the measurement set, in (BARAN, 2012) the power flow and injection measurements are converted into equivalent current measurements. Since branch currents in rectangular coordinates are used, the Jacobian matrix becomes linear. The proposal in (ALMEIDA; OCHOA, 2017) also converts active and reactive power measurements in equivalent current measurements since node voltages in rectangular coordinates are used as state variables and this, in turn, makes it so that the Jacobian matrix is constant between iterations. (PAU; PEGORARO; SULIS, 2013a) presents a comparison in terms of computational performance between formulations that use node voltages or branch currents as state variables. Each of these formulations is also evaluated using polar versus rectangular coordinates. The conclusion is that the Branch Current State Estimator (BCSE) is the fastest, however, certain modifications in the original formulation are necessary to improve accuracy which can decrease performance.

There are alternative WLS formulations that aim to solve one specific drawback associated with virtual measurements: their higher weights compared to other types of measurements can induce ill-conditioning. Some proposals such as (LIN; TENG, 1996) and (THORNLEY; JENKINS; WHITE, 2005) suggest modelling virtual measurements

as equality constraints that are included in the WLS formulation using Lagrangian Relaxation. This, however, produces excessive fill-in and can lead to some numerical instability. Aiming specifically at the ill-conditioning and numerical instability that can occur when factorizing the Gain matrix, (MONTICELLI; MURARI; WU, 1985), (SIMOES-COSTA; QUINTANA, 1981b) and (SIMOES-COSTA; QUINTANA, 1981a) suggest using orthogonal transformations that lead to solving the least-square problem via backwards substitution.

Backwards substitution is a technique used to obtain a solution to a linear system where the matrix of coefficients is upper triangular. Upper or lower triangular systems are obtained via factorization and there are a few methods to choose from. Usually, the Cholesky factorization is applied to the symmetric, positive-definite Gain Matrix when the system is observable. In DS, when the system is observable, the Cholesky factorization can also be applied, however, the Gain matrix can be highly sparse meaning that there are a much larger number of zeros than non-zero elements. Depending on the way that the factorization process is performed, it can create a lot of fill-in, which are non-zero elements in the factors that were originally zero in the matrix being factorized. In addition to the ill-conditioning associated with specifics of DS, fill-in created by the factorization can further decrease the numerical stability of the iterative process required by the WLS estimation.

In summary, the specifics of DSs such as the large number of virtual measurements, three-phase and unbalanced nature among others which have been shown contribute to the ill-conditioning of the associated Gain matrix. When applying the usual techniques used to factorize this matrix, further numerical instability can be induced by the creation of fill-in. Computational performance also suffers because the usual factorization techniques are not fully optimized to deal with the sparse nature of the matrices. The alternatives to the WLS estimator have not been able to sufficiently solve the ill-conditioning issue and with expected increase in data volume there appears to be a need for robust, sparse oriented techniques applied to DSSE in order to obtain a reliable state estimation subject to the constraints of real-time operations.

The objectives and expectations of this work are outlined in the next section.

1.2 Objectives

In light of the previous section, DSs face challenges to the application of the WLS state estimator on one side because of inherent characteristics that result in ill-conditioning of the Gain matrix and on the other side because the usual methods for solving linear systems are not suitable to deal with this higher condition number, resulting in numerical problems. The scope of this work is, therefore, to evaluate the application of sparse-oriented techniques to solve linear systems and the use of a more robust formulation for DSSE

based on orthogonal transformations that allows the application of state-of-the-art solvers to obtain a reliable WLS solution. Test systems from the literature are used with their complete three-phase models and also different measurement sets are built to represent some network conditions that the operators might face.

The state estimator processes an amount of data, which are the available measurements as well as the network topology and parameters, in order to obtain the estimated state that represents the real-time condition of the network. The increase in these available measurements for DSs in the form of smart-meters and other monitored devices means that the amount of data that needs to be processed will increase as well. Since DS can have a large number of nodes and branches, the processing of these large volumes of data needs efficient storage and sparse-oriented techniques to speed up computations and decrease computational effort. This work shows the application of a technique that reorders a matrix before the factorization step necessary in the WLS solution. This, in turn, reduces the number of non-zero elements created in this process maintaining the sparsity of the matrix being factorized. This work presents some of these reordering methods and evaluates them with the test systems.

The sparse techniques are one part in the scope of this work. Another part is the use of robust factorization methods, namely the QR factorization, in order to improve the reliability of the solution and decrease the numerical instability of the WLS estimation process, which is caused by the ill-conditioning of the Gain matrix. This work presents a formulation that uses the numerical properties of the QR factorization to avoid the calculation of the Gain matrix in the WLS state estimation process. In order to extract peak computational performance, a state-of-the-art implementation of the QR factorization is presented and evaluated with the test systems. This implementation takes advantage of the sparse storage and sparse techniques mentioned and it also has other possible improvements in terms of parallelism that can be looked into in the future.

In summary, this work will implement an orthogonal formulation of the WLS state estimator with focus on accuracy and performance. This metrics will be compared with a dedicated DSSE algorithm as well as alternative formulations of the WLS state estimator.

1.3 Work Structure

This work is organized as follows:

Chapter 2 presents the mathematical formulation of the WLS state estimator and definitions for the associated ill-condition of the Gain Matrix. A section is dedicated to present the three phase mathematical models of the components present in DSs. The measurement types present in DSSE as well as their impact on the state estimation are presented in another section. The formulation of the dedicated DSSE algorithm

implemented in this work is also presented as well as the alternatives to the WLS formulation that aim to improve the ill-conditioning of the Gain matrix

Chapter 3 is dedicated to discussing linear system solvers applied to sparse problems. Sparse techniques are presented as well as algorithms to maintain said sparsity during the factorization process. A formal discussion of ill-conditioning and stability is also presented as well as an algorithm dedicated to performing the QR factorization of sparse matrices.

Chapter 4 proposes an orthogonal formulation of the WLS Estimator that avoids the use of the Gain matrix and, in turn, greatly decreases the condition number of the system being factorized. This formulation requires a QR factorization such as the one presented in Chapter 3.

Chapter 5 shows results obtained and presents the test systems used. The majority of the results were obtained with the formulation shown in Chapter 4 as well as the technique presented in Chapter 3. Results obtained with fill-in reducing methods are also present. Comparisons are carried between the proposed orthogonal formulation and the dedicated DSSE algorithm, other WLS formulations are evaluated as well.

Finally, the plans for future works are in Chapter 6. Conclusions are presented as well as the published articles based on this work.

2 DISTRIBUTION SYSTEMS STATE ESTIMATION

In this chapter, the traditional formulation of the WLS state estimator is presented. This formulation is sufficiently generic to be used with three as well as single-phase (positive sequence) models. In this work, the focus is on three phase modelling, therefore, the formulation of the models used for the electrical components are presented in a dedicated section. There is also a section dedicated to presenting the different types of measurements available for DSSE.

A dedicated section presents the Branch Current formulation for DSSE. The necessary approximations are shown as well as the algorithm implemented. Another section extends the presented WLS formulation, showing two alternatives that aim to improve the ill-conditioning of the Gain matrix. The first of these alternatives model virtual measurements as equality constraints and the second, called Augmented Hatched Matrix, includes the measurement residuals as equality constraints in addition to the virtual measurements.

The complete state estimation process can be viewed as a series of steps: the first one is to obtain the topology of the system given information about electrical devices, equipment as well as the state of switches in the network. The second step, called observability analysis, checks if it's possible to obtain all state variables given the available measurements and if it is, the system is called observable. Combining both network topology and available measurements, the third step, which is the focus of this work, performs the necessary calculations in order to obtain the state variables. Finally, there is a fourth step that's called Gross Errors Processing. This step evaluates the estimated state and aims to identify any measurements with gross errors and if any are found, this step eliminates them so that the state variables can be calculated again.

2.1 WLS State Estimator

DSSE is based on the nonlinear model of measurements:

$$z = h(x) + e, \quad (2.1)$$

where z is the measurement vector ($m \times 1$), x is the state variables vector ($n \times 1$), $h(\cdot)$ is the nonlinear state estimation function ($m \times 1$) that relates the measurements to the states variables, and e is the vector of measurement errors ($m \times 1$) usually considered as independent random Gaussian variables with zero mean and diagonal covariance matrix R_z ($R_z = \text{diag} \{ \sigma_{z1}^2, \sigma_{z2}^2, \dots, \sigma_{zm}^2 \}$, where σ_{zi} is the standard deviation of measurement z_i).

Through the classical WLS estimator, the state estimate vector \hat{x} is obtained by

minimizing the index $J(x)$ given by:

$$J(x) = [z - h(x)]^T W [z - h(x)], \quad (2.2)$$

where $W = R_z^{-1}$.

The minimum value for $J(x)$ is obtained when its derivative is equal to zero which can be written as:

$$\frac{\partial J(x)}{\partial x} = 2H^T(\hat{x})W[z - h(\hat{x})] = 0 \quad (2.3)$$

The matrix $H(\hat{x})$ is known as the Jacobian matrix and it is the matrix of first derivatives of $h(x)$ evaluated at the $x = \hat{x}$ point. Given the nonlinear nature of the index $J(x)$, an iterative algorithm is used to obtain a solution to a linear equation, which calculates a correction, Δx^k , to the state vector where k is the iteration index. The linear approximation at the point x^k is:

$$h(x^{k+1}) \approx h(x^k) + H(x^k)\Delta x^k \quad (2.4)$$

Rewriting (2.1) considering the linear approximations presented beforehand we obtain:

$$z = h(x^k) + H(x^k)\Delta x^k + e \quad (2.5)$$

Which is equivalent to:

$$\Delta z(x^k) = z - h(x^k) = H(x^k)\Delta x^k + e \quad (2.6)$$

From the linear approximations, it is possible to write a new objective function $J(\Delta x)$:

$$J(\Delta x) = [\Delta z(x^k) - H(x^k)\Delta x^k]^T W [\Delta z(x^k) - H(x^k)\Delta x^k] \quad (2.7)$$

The minimum of $J(\Delta x)$ is obtained when:

$$\frac{\partial J(\Delta x)}{\partial x} = 2H(x^k)^T W [\Delta z(x^k) - H(x^k)\Delta x^k] = 0 \quad (2.8)$$

The correction Δx^k is then given by the solution of:

$$\Delta x^k = [H(x^k)^T W H(x^k)]^{-1} H(x^k)^T W \Delta z(x^k) \quad (2.9)$$

Equation 2.9 is known as the *Normal Equation* and to obtain its solution it's necessary to invert, or more commonly, factorize $H(x^k)^T W H(x^k)$ which is called the Gain Matrix.

Since this work focuses on three phase networks and models, for the state estimation of a distribution system with n_{nodes} and n_{phases} , the state variables are defined as:

$$x = [V_\phi^p \ \theta_\phi^p] \quad p \in \{1, \dots, n_{nodes}\}; \quad \phi \in \{1, \dots, n_{phases}\} \quad (2.10)$$

The nonlinear state estimation function $h(x)$ represents the available measurements in terms of the state variables. These measurements can be active and reactive power flow in a branch, active and reactive power injections in a node and voltage magnitude also in a node. The following model presents all these measurement types, the subscript km means active (P) or reactive (Q) power flow in the branch connecting nodes k to m and the single subscript k means either and active or reactive power injection or voltage magnitude (V) at node k .

$$h(x) = \begin{pmatrix} P_{\phi}^{km}(x) \\ Q_{\phi}^{km}(x) \\ P_{\phi}^k(x) \\ Q_{\phi}^k(x) \\ V_{\phi}^k(x) \end{pmatrix} \quad (2.11)$$

The aforementioned WLS state estimator requires the calculation of the Jacobian matrix $H(x)$ which is the matrix of first derivatives of the nonlinear measurement model $h(x)$. Taking into account the possible measurement types as presented in equation 2.11, the Jacobian matrix can be constructed as follows:

$$H(x) = \begin{pmatrix} \frac{\partial P_{\phi}^{km}(x)}{\partial V_{\phi}^k} & \frac{\partial P_{\phi}^{km}(x)}{\partial \theta_{\phi}^k} \\ \frac{\partial Q_{\phi}^{km}(x)}{\partial V_{\phi}^k} & \frac{\partial Q_{\phi}^{km}(x)}{\partial \theta_{\phi}^k} \\ \frac{\partial P_{\phi}^k(x)}{\partial V_{\phi}^k} & \frac{\partial P_{\phi}^k(x)}{\partial \theta_{\phi}^k} \\ \frac{\partial Q_{\phi}^k(x)}{\partial V_{\phi}^k} & \frac{\partial Q_{\phi}^k(x)}{\partial \theta_{\phi}^k} \\ \frac{\partial V_{\phi}^k(x)}{\partial V_{\phi}^k} & 0 \end{pmatrix} \quad (2.12)$$

The nonlinear equations and its derivatives requires the modelling of the components of the DS, in this work specifically, the three-phase models are used.

2.2 Three Phase Models

The three-phase network modelling to perform DSSE in this work consists on the representation of each element of the DS by its two-port admittance matrix. Different types of equipment and connections can be incorporated in the measurement model by simply changing the respective admittance matrix, which is an implementation advantage when representing complex distribution networks with several different components (AHMAD *et al.*, 2018b). Each element is modelled by the following two-port model (HEBLING *et al.*, 2020):

$$\begin{pmatrix} \dot{I}_k \\ \dot{I}_m \end{pmatrix} = \begin{pmatrix} Y_{kk} & Y_{km} \\ Y_{mk} & Y_{mm} \end{pmatrix} \cdot \begin{pmatrix} \dot{V}_k \\ \dot{V}_m \end{pmatrix}, \quad (2.13)$$

where, k and m denote the terminals of the branch element, \dot{I}_k and \dot{I}_m are the current phasor injected in each terminal of the branch element, \dot{V}_k and \dot{V}_m the voltage phasor of each terminal, and Y_{kk} , Y_{km} , Y_{mk} and Y_{mm} are the 3×3 admittance sub-matrices that represent each equipment and the respective parameters.

The power flow equations can be written for the respective branch as the following matrix expression for the terminal k :

$$S_{km} = P_{km} + j.Q_{km} = \dot{V}_k \odot (\dot{I}_k)^* = \dot{V}_k \odot (Y_{kk} \cdot \dot{V}_m + Y_{km} \cdot \dot{V}_m)^*, \quad (2.14)$$

where, S_{km} is a vector with the per-phase complex power at terminal k (active and reactive power flows, P_{km} and Q_{km}), \odot denotes the Hadamard product (element-wise), and $*$ denotes the complex conjugate. Separating the voltage phasor in its exponential representation according to the following expression:

$$\dot{V}_k = V_k \odot \theta_k = \text{diag}(V_k) \cdot \theta_k = [V_k] \cdot \theta_k, \quad (2.15)$$

where $[\cdot]$ denotes, for the sake of notation simplification, a diagonal matrix formed by the elements of a vector. As an example, for a three-phase terminal k with phases abc , the following equation can be written through the matrix notation of the two-port model and the above product:

$$S_{km} = \dot{V}_k \odot (\dot{I}_k)^* = \begin{pmatrix} \dot{V}_k^a (\dot{I}_k^a)^* \\ \dot{V}_k^b (\dot{I}_k^b)^* \\ \dot{V}_k^c (\dot{I}_k^c)^* \end{pmatrix} = \text{diag}(\dot{V}) (\dot{I}_k)^* = \begin{pmatrix} \dot{V}_k^a & 0 & 0 \\ 0 & \dot{V}_k^b & 0 \\ 0 & 0 & \dot{V}_k^c \end{pmatrix} \begin{pmatrix} (\dot{I}_k^a)^* \\ (\dot{I}_k^b)^* \\ (\dot{I}_k^c)^* \end{pmatrix} \quad (2.16)$$

Expanding the power flow matrix expression, it is possible to obtain the classical active and reactive power flow equations for a three-phase component (ARRILLAGA; HARKER, 1978):

$$P_{km}^i = V_k^i \sum_{j \in \Phi_{km}} V_k^j \left(g_{kk}^{ij} \cos(\theta_k^i - \theta_k^j) + b_{kk}^{ij} \sin(\theta_k^i - \theta_k^j) \right) - V_m^j \left(g_{km}^{ij} \cos(\theta_k^i - \theta_m^j) + b_{km}^{ij} \sin(\theta_k^i - \theta_m^j) \right) \quad (2.17)$$

$$Q_{km}^i = V_k^i \sum_{j \in \Phi_{km}} V_k^j \left(g_{kk}^{ij} \sin(\theta_k^i - \theta_k^j) - b_{kk}^{ij} \cos(\theta_k^i - \theta_k^j) \right) - V_m^j \left(g_{km}^{ij} \sin(\theta_k^i - \theta_m^j) - b_{km}^{ij} \cos(\theta_k^i - \theta_m^j) \right) \quad (2.18)$$

where, i and j denote different phases of the component; g_{kk}^{ij} and b_{kk}^{ij} are the real and imaginary parts of the ij element from the two-port model submatrix Y_{kk} ; g_{km}^{ij} and b_{km}^{ij}

are the real and imaginary parts of the ij element from the two-port model submatrix Y_{km} ; Φ_{km} is the set of existing phases at branch k - m .

In order to build the Jacobian matrix presented in Equation 2.12, it's necessary to calculate the derivatives of power flow and power injection measurements. Since the derivative of a power injection at node k can be calculated as the sum of the power flows from node k to all its adjacent nodes, only the power flow derivative are presented, for state variables as node voltages they are as follows:

$$\begin{aligned} \frac{\partial S_{km}}{\partial V_k^i} &= J^{ii}[\theta_k]Y_{kk}^*[V_k]\theta_k^* + [V_k][\theta_k]Y_{kk}^*J^{ii}\theta_k^* + J^{ii}[\theta_k]Y_{km}^*[V_m]\theta_m^* \\ \frac{\partial S_{km}}{\partial V_k^i} &= [V_k][\theta_k]Y_{km}^*J^{ii}\theta_m^* \end{aligned} \quad (2.19)$$

$$\frac{\partial S_{km}}{\partial \theta_k^i} = je^{\theta_k^i}[V_k]J^{ii}Y_{kk}^*[V_k]\theta_k^* - j[V_k][\theta_k]Y_{kk}^*[V_k]J^{ii}\theta_k^* + je^{\theta_k^i}[V_k]J^{ii}Y_{km}^*[V_m]\theta_m^*$$

$$\frac{\partial S_{km}}{\partial \theta_m^i} = -j[V_k][\theta_k]Y_{km}^*[V_m]J^{ii}\theta_m^* \quad (2.20)$$

where, J^{ii} is a matrix with the same size as the number of phases and only the ii element equal one and the others equal zero. The above equation yields derivatives for all phases of the active and reactive power flow at once.

It is noteworthy that the above equations can be used for different types of equipment, connections and number of phases, composing a general model for steady state analysis such as DSSE. In this work, the modelling of the electrical circuits and transformers for a three-phase abc system will be presented.

2.2.1 Power lines and Transformers

Using Carson's equations (KERSTING, 2001), it is possible to obtain the parameters of the cables so that the behaviour of the electrical and magnetic fields through the lines are correctly represented. The three-phase branches are, therefore, represented using impedance matrices with series as well as shunt components. Figure 1 shows a three-phase branch with the electrical parameters necessary to build the two-port model.

The two-port model for the three-phase branch shown in Figure 1 is as follows:

$$Y^{kk} = Y^{mm} = Z_{series}^{-1} + Y_{shunt} \quad (2.21)$$

$$Y^{km} = Y^{mk} = -Z_{series}^{-1} \quad (2.22)$$

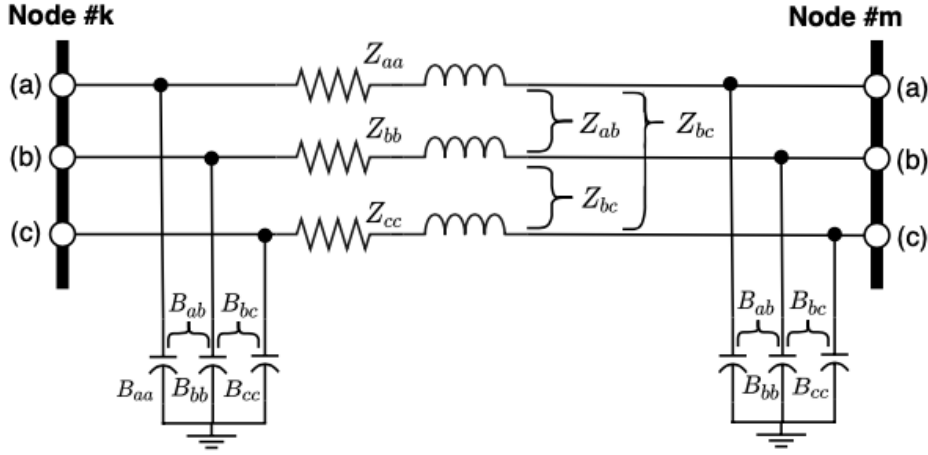


Figure 1 – Three-phase branch circuits. The impedance and capacitancy self parameters ($Z_{aa}, B_{aa}, Z_{bb}, B_{bb}, Z_{cc}, B_{cc}$) as well as mutual parameters ($Z_{ab}, B_{ab}, Z_{bc}, B_{bc}, Z_{ca}, B_{ca}$) are given by specific characteristic of the cables. Source: Author

The impedance matrix Z_{series} contains the series elements of the circuit, following the notation presented in Figure 1:

$$Z_{series} = \begin{pmatrix} R_{aa} + j.X_{aa} & R_{ab} + j.X_{ab} & R_{ac} + j.X_{ac} \\ & R_{bb} + j.X_{bb} & R_{bc} + j.X_{bc} \\ & & R_{cc} + j.X_{cc} \end{pmatrix} \quad (2.23)$$

The shunt elements are represented by the matrix Y_{shunt} , which contains the following:

$$Y_{shunt} = \begin{pmatrix} j.B_{aa} & j.B_{ab} & j.B_{ac} \\ & j.B_{bb} & j.B_{bc} \\ & & j.B_{cc} \end{pmatrix} \quad (2.24)$$

2.2.2 Transformers

Transformers are a central equipment in DS. They are responsible for regulating the voltage levels across the network in order to deliver the energy safely to the end consumers. Transformers connect the DS with the sub-transmission system, safely interfacing voltage levels. Within the network, these devices are also responsible for the connection between the primary and secondary networks which operate in the medium and low voltage respectively. Different connection windings present in the network are represented by different matrices in the two-port model. The connections of the primary and secondary windings can be Delta (D), Wye (W) and Grounded Wye (Gw) for a total of 9 possible combinations. Each combinations has a different formulations for the submatrices Y^{kk} , Y^{mm} , Y^{km} and Y^{mk} and these formulations are shown in Table 1.

Connection type		Submatrices			
Primary	Secondary	Y^{kk}	Y^{mm}	Y^{km}	Y^{mk}
Gw	Gw	$\alpha^2.Y_I$	$\beta^2.Y_I$	$-\alpha.\beta.Y_I$	$-\alpha.\beta.Y_I$
Gw	W	$\alpha^2.Y_{II}$	$\beta^2.Y_{II}$	$-\alpha.\beta.Y_{II}$	$-\alpha.\beta.Y_{II}$
Gw	D	$\alpha^2.Y_I$	$\beta^2.Y_{II}$	$\alpha.\beta.Y_{III}$	$\alpha.\beta.Y_{III}^T$
W	Gw	$\alpha^2.Y_{II}$	$\beta^2.Y_{II}$	$-\alpha.\beta.Y_{II}$	$-\alpha.\beta.Y_{II}$
W	W	$\alpha^2.Y_{II}$	$\beta^2.Y_{II}$	$-\alpha.\beta.Y_{II}$	$-\alpha.\beta.Y_{II}$
W	D	$\alpha^2.Y_{II}$	$\beta^2.Y_{II}$	$\alpha.\beta.Y_{III}$	$\alpha.\beta.Y_{III}^T$
D	Gw	$\alpha^2.Y_{II}$	$\beta^2.Y_I$	$\alpha.\beta.Y_{III}$	$\alpha.\beta.Y_{III}^T$
D	W	$\alpha^2.Y_{II}$	$\beta^2.Y_{II}$	$\alpha.\beta.Y_{III}^T$	$\alpha.\beta.Y_{III}$
D	D	$\alpha^2.Y_{II}$	$\beta^2.Y_{II}$	$-\alpha.\beta.Y_{II}$	$-\alpha.\beta.Y_{II}$

Table 1 – Submatrices of the two-port model based on the different connection type of the windings

In Figure 2, the connections between primary and secondary windings are shown. The two-port model for this specific transformer can be obtained with the formulation in Table 1. The parameters α and β are the primary and secondary taps which are either fixed or variable in the case of voltage regulators. The matrices Y_I , Y_{II} and Y_{III} are based on the admittance y_t , as shown in Figure 2, and are build using equation 2.25.

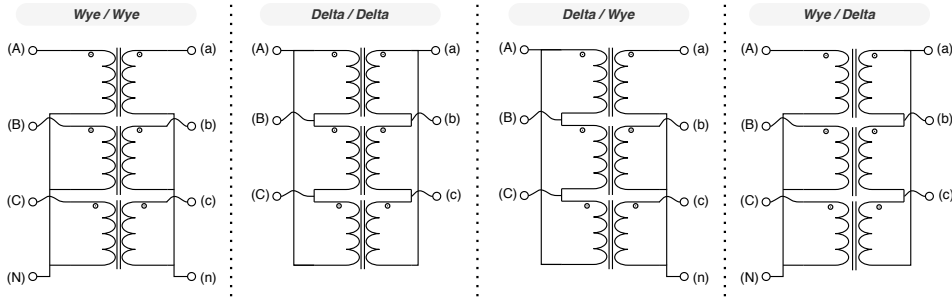


Figure 2 – Three-phase transformer connections of the primary and secondary windings. Source: Author.

$$Y_I = y_t \cdot \begin{pmatrix} 1 & 0 & 0 \\ 0 & 1 & 0 \\ 0 & 0 & 1 \end{pmatrix} \quad Y_{II} = \frac{y_t}{3} \cdot \begin{pmatrix} 2 & -1 & -1 \\ -1 & 2 & -1 \\ -1 & 2 & -2 \end{pmatrix} \quad Y_{III} = \frac{y_t}{\sqrt{3}} \cdot \begin{pmatrix} -1 & 1 & 0 \\ 0 & -1 & 1 \\ 1 & 0 & -1 \end{pmatrix} \quad (2.25)$$

Details of three-phase models and respective admittance matrices to build each two-port model for other equipment that are present in DSs such as voltage regulators, capacitor banks among others can be found in (LOURENÇO E. M.; LONDON JR., 2022)

In addition to the three-phase models that directly impact the nonlinear formulations of the WLS, DSs can have different measurement types with varying precision. This variation is one of the causes of ill-condition is DSSE, as is the case with virtual

measurements that have a high weight associated with them. Understanding the differences between the measurements is essential to the characterization of DSSE as a whole and the next section is dedicated to presenting the specifics of each measurement type.

2.3 Measurement Types

The measurement vector z aggregates all measurements available in the network. The state estimator will then process all these measurements and its result will be the estimated state of the network. In order to obtain a reliable estimate and also to guarantee that the system is observable, a redundant set of measurements is necessary and these can be characterized in one of three: real-time, pseudo or virtual measurements.

Supervisory Control and Data Acquisition (SCADA) systems gather the Real-time measurements that consists of monitored electrical quantities in the system which are typically power flows, power injections, voltage and current magnitudes across the network. Usually, the information given by the SCADA systems is updated every few seconds. Another recent source of information in DSs is the smart meter: a device that has started to be widely deployed in the low voltage networks. These smart meters typically provide power injections and voltage magnitudes at a consumer level and report the demand data every 15 or more minutes. Another important kind of measurements are the synchronized phasor measurements obtained by Phasor Measurement Units (PMUs) which monitor the voltage and current phasor (magnitude and angle) and these can have a variable rate of messages sent, from 1 to 60 per second.

Pseudo measurements are usually active and reactive power injections in the distribution transformers. These measurements are built using typical load curves, energy consumption data, load profiles and climate data. Nowadays, pseudo measurements are the majority of information available about the operational state of the DSs and their qualities have a direct impact on the DSSE accuracy (MASSIGNAN *et al.*, 2018). These pseudo measurements are necessary in such large quantities, in relation to other types of measurements, to ensure the observability of the system and enable the application of state estimation (PRIMADIANTO; LU, 2017). In order to generate these kind of pseudo measurements, consumers are divided into classes: residential, commercial or industrial. Each class has a typical load pattern associated and a statistical process is used to obtain a load curve which will, then, generate the pseudo measurement for a given time of day. Historical data can also be used to generate pseudo measurements and the weights associated with these generated measurements are lower when compared with the other types of measurements

Virtual measurements represent known electrical quantities in the system such as zero-injection nodes (nodes without loads or generation) and are incorporated as measurements with low standard deviations. This is because these measurements are

known electrical quantities despite there being no actual meter present. The differences among the variance values of the real-time, virtual and pseudo-measurements are another well-known source of ill-conditioning in DSSE (LIN; TENG, 1996; THORNLEY; JENKINS; WHITE, 2005) and also an essential motivation for using a stable approach such as the method proposed in this work. It is noteworthy that other approaches may also be applied for dealing with virtual measurements, such as using equality constraint formulation by Lagrangian methods for DSSE (LIN; TENG, 1996).

2.4 Alternative WLS formulations

The ill-conditioning of the Gain matrix motivated researchers to develop modification on the WLS formulation in order to improve the robustness of the estimation, mainly in the presence of a large number of virtual measurements. Since these measurements have a larger weight associated to them, as they are known zero quantities in the network, the discrepancy between higher and lower measurement weights compromises the numerical stability of the solution because the measurement weights are the diagonal elements of R^{-1} , that is, the weight of a measurement is the inverse of its variance.

2.4.1 WLS with Equality Constraints

The first alternative formulation of the WLS estimator includes virtual measurements as a constraint to the following optimization problem:

$$\begin{aligned} \min \quad & J(x) = [z - h(x)]^T R^{-1} [z - h(x)] \\ \text{s.t.} \quad & c(x) = 0 \end{aligned} \quad (2.26)$$

where $c(x)$ is the vector of non-linear equations which represent the zero power injections. Using the Lagrangean function, it's possible to rewrite the optimization problem as the following, where λ is the vector of Lagrangean multipliers:

$$\mathcal{L}(x, \lambda) = [z - h(x)]^T R^{-1} [z - h(x)] - \lambda^T c(x) \quad (2.27)$$

Applying the first order optimality conditions, the following system of derivatives is obtained:

$$\begin{aligned} \frac{\partial \mathcal{L}(x, \lambda)}{\partial x} = 0 &\Rightarrow H^T(x) R^{-1} [z - h(x)] + C^T(x) \lambda = 0 \\ \frac{\partial \mathcal{L}(x, \lambda)}{\partial \lambda} = 0 &\Rightarrow c(x) = 0 \end{aligned} \quad (2.28)$$

In this system of equations, $C(x) = \frac{\partial c(x)}{\partial x}$ is the vector of first derivatives of the non-linear equations of the vector $c(x)$ with respect to the vector of state variables x . In

the same way as the WLS state estimator formulation, an iterative method is applied to obtain a correction for the state variables at each step which requires the solution of the following:

$$\begin{aligned} H^T R^{-1}[z - h(x^k) - H(x^k)\Delta x^k] + C^T(x^k)\lambda^k &= 0 \\ c(x^k) + C(x^k)\Delta x^k &= 0 \end{aligned} \quad (2.29)$$

In matrix form, the system becomes:

$$\begin{bmatrix} H^T(x^k)R^{-1}H(x^k) & C^T(x^k) \\ C(x^k) & 0 \end{bmatrix} \cdot \begin{bmatrix} \Delta x^k \\ -\lambda^k \end{bmatrix} = \begin{bmatrix} H^T(x^k)R^{-1}[z - h(x^k)] \\ -c(x^k) \end{bmatrix} \quad (2.30)$$

In order to solve this linear system, it's necessary to pivot the rows of the coefficient matrix during the factorization. A 2 x 2 pivoting is recommended to improve numerical stability (GJELSVIK; AAM; HOLTEN, 1985). Although the conditioning of the coefficient matrix improves, because the larger weights associated with virtual measurements are removed from the matrix R^{-1} , this formulation does not completely solve the ill-conditioning problem. It's possible to reduce the ill-conditioning of the system by applying a scaling factor in equation 2.27. This equation then becomes:

$$\mathcal{L}(x, \lambda) = [z - h(x)]^T R^{-1}[z - h(x)] - \lambda_s^T c(x) \quad (2.31)$$

where $\lambda_s^T = \alpha \lambda^T$ and α is a scalar that can be chosen as:

$$\alpha = \frac{1}{\max\{R_{ii}^{-1}\}} \quad \text{or} \quad \alpha = \frac{m}{\sum_{i=1}^m R_{ii}^{-1}} \quad (2.32)$$

Other factors inherent to DSs and not related to the presence of virtual measurements still affect the condition number of the Gain matrix, mainly related to the topology of the network as was previously discussed. Therefore, this formulation may not solve entirely the ill-condition problem of the Gain matrix. Also, the addition of equality constraints increases the size of the linear system that needs to be solved which may impact computational performance for larger systems.

2.4.2 Hatchel Augmented Matrix Method

The Hatchel Augmented Matrix Method extends the formulation of the WLS with Equality Constraints by considering the vector of residuals r in the optimization problem, such as:

$$\begin{aligned}
\min \quad J(x) &= [z - h(x)]^T R^{-1} [z - h(x)] \\
\text{s.t. :} \quad c(x) &= 0, \\
r - z + h(x) &= 0
\end{aligned} \tag{2.33}$$

Using the Lagrangean function, it's possible to rewrite the objective function as:

$$\mathcal{L}(x, r, \lambda, \mu) = [r^T R^{-1} r] - \lambda^T c(x) - \mu^T [r - z + h(x)] \tag{2.34}$$

Where, analogous to the previous formulation, λ and μ are Lagrange multipliers. The first one is associated with the virtual measurements constraint and the second is associated with the residuals constraint. Applying the first order optimality condition, the following derivatives are obtained:

$$\begin{aligned}
\frac{\partial \mathcal{L}(x, r, \lambda, \mu)}{\partial x} &= 0 \Rightarrow C^T(x)\lambda + H^T(x)\mu = 0 \\
\frac{\partial \mathcal{L}(x, r, \lambda, \mu)}{\partial r} &= 0 \Rightarrow R^{-1}r - \mu = 0 \\
\frac{\partial \mathcal{L}(x, r, \lambda, \mu)}{\partial \lambda} &= 0 \Rightarrow c(x) = 0 \\
\frac{\partial \mathcal{L}(x, r, \lambda, \mu)}{\partial \mu} &= 0 \Rightarrow r - z + h(x) = 0
\end{aligned} \tag{2.35}$$

The second derivative, $\frac{\partial \mathcal{L}(x, r, \lambda, \mu)}{\partial r}$, simplifies to $r = \mu R$ which eliminates this variable. The linear system to be solved becomes:

$$\begin{bmatrix} R & H(x^k) & 0 \\ H^T(x^k) & 0 & C^T(x^k) \\ 0 & C(x^k) & 0 \end{bmatrix} \cdot \begin{bmatrix} \mu^k \\ \Delta x^k \\ -\lambda^k \end{bmatrix} = \begin{bmatrix} [z - h(x^k)] \\ 0 \\ -c(x^k) \end{bmatrix} \tag{2.36}$$

In order to solve this linear system a factorization method is applied. A 2 x 2 pivoting is recommended to improve numerical stability, similar to the WLS formulation with Equality Constraints. The formulation in 2.36 is able to reduce even further the condition number of the coefficient matrix, however, it becomes larger and more sparse and efficient factorization algorithms are necessary to maintain computational performance.

2.5 Dedicated Distribution System State Estimators

Given the context presented, the usual state estimators applied to transmission systems such as the WLS estimator presented, face challenges when applied to DSs. There

is an increasing need for monitoring of the DS with the development of *Smart Meters* and *Smart Grids* and the utilities rely on the state estimator to provide the operational condition of the network which is then used as a starting point for other static analysis tools. The complexities related to DS motivated researches to develop dedicated state estimators with different formulations, for example, using branch currents in rectangular form as state variables. In this section, some of these formulations will be presented as well as their limitations and strenghts.

2.5.1 Branch-Current State Estimator

The Branch-Current State Estimator is based on the WLS formulation presented in equation 2.1. Instead of node voltages in polar coordinates, currents flowing in the branches in rectangular form are used as state variables. This decouples the phases and also reduces ill-conditioning problems (BARAN; MCDERMOTT, 2009).

In order to exploit a linear relationship between the measurement model and the state variables, the vector z is converted in equivalent current measurements. (BARAN, 2012) assumes that actual power measurements and/or pseudomeasurements are available. Real and imaginary parts of the equivalent current measurement at a node m are:

$$I_r^m + jI_x^m = \frac{P^m + jQ^m}{V^m} \quad (2.37)$$

where the subscripts r and x denote the real and imaginary part, respectively. P^m and Q^m are either active and reactive power injections at node m or active and reactive power flows originating from node m to its adjacent nodes. V^m is the complex voltage. Transforming the measurement vector using 2.37 allows the Jacobian matrix to be constant. Its elements are either 1, -1 or zero.

The estimated state x can then be obtained in a single step, solving:

$$H^T R^{-1} H x = H^T R^{-1} z \quad (2.38)$$

where H is the Jacobian matrix and z is the equivalent measurement vector.

Even though the currents can be obtained by solving equation 2.38 the entire Branch Current estimation process requires more steps. First, in order to calculate the equivalent current measurements, the node voltages need to be initialised. Then, the branch currents can be estimated using equation 2.38 and these estimated currents are used to updated the node voltages using the forward sweep method. These steps are performed until convergence is obtained which means a low enough difference between estimated currents from two iterations.

In order to exploit the computational performance from having a constant Jacobian matrix, only power flow and injections measurements are used. When current or voltage

measurements are included, the Jacobian matrix becomes non-linear and an iterative process is required to obtain the estimated currents x . Including the information of the voltage at the substation, that is, a voltage measurement of the reference node can improve the quality of the estimation (PAU; PEGORARO; SULIS, 2013b).

Another important aspect of the Branch Current state estimator is that it is better suited for radial networks. Even though distribution system networks are usually radial, some meshes can occur and the application of the estimator in this weakly meshed networks requires the addition of an equality constraint in the formulation. This constraint represents the Kirchoff's Voltage Laws applied to the closed loop in the network. In the presence of loops, the estimated vector x is obtained via an iterative process and the phases become coupled. Both changes can negatively impact the computational performance.

2.5.2 Admittance Matrix Based State Estimator

This estimator is based on the WLS formulation presented in 2.1. The measurement vector z , however, contains equivalent currents and voltages in rectangular form. The state variables are node voltages also in rectangular form, therefore, the Jacobian matrix corresponds to the Admittance matrix of the system and is constant. The constant matrix is achieved if the variances of the equivalent measurements are considered constant, which is an approximation (LIN; TENG, 1996).

The equivalent measurements are obtained by converting active and reactive power measurements in real and imaginary equivalent currents and voltage measurements in complex equivalent voltages and they are updated at each iteration of the estimator. Voltages are initialised as a *flat start* and a correction is obtained by solving a normal equation similar to equation 2.9. Convergence is obtained when the voltage difference between iterations falls below a predetermined tolerance.

Voltage magnitude measurements are converted to equivalent complex voltages which can lead to convergence problems. Also, since the real and the imaginary part of the equivalent complex voltage are considered as separate measurements, the total number of available measurements is artificially increased. The imaginary part of the equivalent measurement can be discarded as proposed in (ALMEIDA; SCHINCARIOL; OCHOA, 2015), however this can only be applied to the one-phase estimator. (ALMEIDA; OCHOA, 2017) proposes an estimator that deals with virtual measurements without associated larger weights and proposes a different method for obtained the equivalent voltage measurements for three-phase DSSE with the goal of improving convergence.

In terms of computational performance, the Branch Current formulation has proven to be better than the AMB (PAU; PEGORARO; SULIS, 2013b) even though both have constant coefficient matrices. Contrary to the Branch Current estimator, the AMB estimator can be applied to weakly meshed networks without further modifications but

there are approximations in this formulation and some convergence difficulties may occur, requiring extensions.

2.6 Summary

This chapter presented the topics necessary to characterize DSSE. The WLS state estimator formulation was presented which calculates the Gain matrix and solve a linear system in order to obtain the next estimated state x^k . The Gain matrix is calculated using the matrix of weights associated with the measurements as well as the Jacobian matrix which is the matrix of first derivatives of the non-linear measurement model with respect to the state variables. The non-linear model that relates the measurement set with the state variables contains the three-phase representations of the electrical equipment such as electrical circuits, transformers and others that may be part of DSs. In this work these equipment are modelled using three-phase two-port model as was shown in the previous sections. The three-phase, two-port model is adopted first because it constitutes a sufficiently general model for different equipment or transformer connections that may be present in DSs and second because of ease of implementation, given its matrix nature.

The different types of measurements usually used in DSSE were presented. SCADA, pseudo and virtual measurements may be available to DSs operators to perform the state estimation. These different types of measurements can impact the conditioning of the Gain matrix given their difference in weight: pseudo measurements have a lower weight, but may be present in large numbers in order to provide observability, whereas virtual measurements have a much higher weight associated with them because they represent known zero quantities in the network. This discrepancy in weights may cause ill-conditioning in the Gain matrix.

There are alternative formulations that aim to improve the ill-conditioning of the Gain matrix. These formulations treat virtual measurements as equality constraints removing the larger weights associated with them. The Hatchel Augmented Matrix Formulation extends this concept further by adding the residual in the formulation which decreases the condition number even further. On the other hand, however, these formulations increase size and sparsity of the coefficient matrix which may require efficient techniques to solve the linear systems.

Dedicated state estimators were proposed to DSs. These estimators rely on approximations and simplifications in order to counter the obstacles that the WLS state estimator faces. The Branch-Current State Estimator uses currents in rectangular form as state variables, which enables it to decouple the phases as well as making the Jacobian matrix linear. Another formulation presented is based on the Admittance Matrix and uses node voltages in rectangular form. These formulations have advantages in terms of computational performance, mainly because the coefficient matrix becomes constant,

however, because of the simplification made these estimators solve an approximate problem which may not correspond to the original WLS formulation.

In summary, obtaining the estimated state of a DS with the WLS estimator requires the solution of a linear system that may be ill-conditioned because of various factors. The next chapter will present factorization methods and sparse techniques that may be used in DSSE.

3 THE PROPOSED ORTHOGONAL WLS STATE ESTIMATOR

3.1 Motivation

The main issue for the application of the WLS State Estimator in DSs is the ill-conditioning of the Gain matrix which can impact the estimation process as well as the numerical quality of the solution. Besides the inherent tendency of the normal equation to ill-conditioning, other factors pertaining to DSs contribute to it: the three-phase unbalanced nature, connections between long and short lines, the presence of virtual measurements as well as other factors regarding the topology of DSs which were previously mentioned.

The measurement set can also impact the condition number of the Gain matrix: larger weights are associated with virtual measurements because they represent known quantities in the network. These higher weights mean lower standard deviations in the matrix R_z in relation to the other types of measurements. Such disparities between weights can lead to ill-conditioning and there are proposals that model these virtual measurements as equality constraints (LIN; TENG, 1996; THORNLEY; JENKINS; WHITE, 2005).

Recall that the Normal Equation requires the factorization of the Gain matrix, given by $H(x^k)^T W H(x^k)$ where H is the Jacobian matrix evaluated at the point x^k and $W = R_z^{-1}$. The aforementioned factors regarding the particularities of DSs can impact the condition number of the Jacobian matrix and this, in turn, greatly impacts the condition number of the Gain matrix. It is possible to show that, if $A = F^T F$, the condition number of A is:

$$K(A) = \frac{\lambda_{max}(A)}{\lambda_{min}(A)} \approx K(F)^2 \quad (3.1)$$

Therefore, if the Jacobian matrix is slightly ill-conditioned, the Gain matrix will be ill-conditioned. In cases where the Jacobian matrix is already ill-conditioned, high condition numbers can be expected for the Gain matrix meaning it will be ill-conditioned. More details about the condition number will be presented further.

Obtaining the estimated state in a DS requires the solution of a possibly ill-conditioned system. Usual factorization methods are not prepared to deal with such systems in a stable way. In this chapter, the theoretical background of linear systems and how to solve them is presented as well as a technique to reduce fill-in during the factorization process. A brief discussion of error analysis is presented in order to introduce the Multifrontal QR algorithm which is used in this work's proposed estimator.

3.2 Sparse Linear Systems

The previous chapter presented the traditional formulation of the WLS state estimator as well as the specifics of its application to three phase distribution networks. Since the estimated state is obtained via an iterative process, at each step it is necessary to solve a linear system. The focus of this section is on the problems faced at the linear factorization step of the WLS state estimator, when the Gain matrix must be factorized to obtain the correction of the state vector. An overview of the condition number is given which can greatly impact the quality of the solution, that is, the estimated state. Special focus is given to ordering methods which are used to maintain the sparse structure of the matrix being factorized and are specially useful in problems such as DSSE where matrices are highly sparse. Finally, there is a section dedicated to the more commonly used factorization methods, their algorithms and mathematical formulations.

3.2.1 Theoretical Background

The state estimation process, using the WLS state estimator formulation, requires the solution of the linear system given by equation 2.9, also called the Normal equation. This system can become ill-conditioned because of the specific characteristics of distribution systems as previously mentioned. The condition number K of a matrix A can be defined as:

$$K(A) = \|A\| \|A^{-1}\| \quad (3.2)$$

Where $\|\cdot\|$ is the euclidean norm. This number represents how close a matrix is to singularity. A perfectly conditioned matrix would have a condition number of 1, whereas a singular matrix has an infinite condition number. When using the Euclidian norm, (QUARTERONI; SACCO; SALERI, 2000) shows that the condition number can be expressed as:

$$K(A) = \frac{\lambda_{max}(A)}{\lambda_{min}(A)} \quad (3.3)$$

where λ_{max} is the largest eigenvalue and λ_{min} is the smallest eigenvalue.

A large condition number implies a greater sensitivity of the solution of the linear system to small perturbations in the inputs. Small errors caused by floating point calculations can result in much larger distortions in the result vector. In order to solve the Normal equation, it is necessary to invert or factorize the Gain matrix. Inverting the Gain matrix is too costly in terms of computational effort and, because of the ill-conditioning, errors and numerical problems could be induced. Factorization methods are then applied and these methods perform operations on the matrix in order to obtain a lower, or upper, triangular system. An upper, or lower, triangular matrix, is a matrix that has all non-zero elements below, or above, the main diagonal.

The triangular system can then be solved using forwards or backwards substitution, for upper and lower systems respectively. Considering the linear system $Lx = b$ where L is

lower triangular, forwards substitution algorithm gives each element of vector x by:

$$x_i = \frac{(b_i - \sum_{j=1}^{i-1} L_{ij}x_j)}{L_{ii}} \quad (3.4)$$

Upper triangular systems, however, can be solved via backwards substitution. Considering the system $Ux = b$, where U is upper triangular, its solution is given by:

$$x_i = \frac{(b_i - \sum_{j=i+1}^n U_{ij}x_j)}{U_{ii}} \quad (3.5)$$

When dealing with dense matrices, which are those that have a lot of non-zero elements, the solution to the linear system boils down to the factorization, since the substitution step is quite straightforward. Sparse matrices, however, may demand a few more steps in order to obtain a solution when computational performance is desired. These steps aim to preserve sparsity, as is the case of the ordering methods which will be presented in the next section, or increase efficiency even further with additional structures and operations specific to sparse matrices.

In the next sections, it will be presented an overview of the most commonly used methods for obtaining the factorization of Gain matrix in the Normal equation as well as a QR factorization that has a property that is central to the topic of this work. In addition to factorization methods, ordering algorithms are presented in a dedicated section. Normally applied as a step before the proper factorization, these reordering methods reduce the number of fill-in elements and decrease memory usage.

3.2.2 Linear System Solvers

A linear system is a set of equations that can be written in matrix format as:

$$Ax = b \quad (3.6)$$

where A is the coefficient matrix, b is a column vector and x is a column vector of the variables to be determined. This system admits a solution if A is invertible which follows that the solution x is given by:

$$x = A^{-1}b \quad (3.7)$$

Computing the inverse of a matrix is, however, far too costly in terms of computational effort. When dealing with large systems factorization methods are preferred so that the solution can be obtained by forwards and/or backwards substitution using equations 3.4 and 3.5. There are two classes of methods for solving linear systems, direct methods that factorize the matrix A in equation 3.6 and iterative methods that aim to obtain successive approximations at every iteration. In this work, only direct methods will be discussed and applied. In order to exist a unique solution to the linear system, the matrix A has to be invertible, which means that its determinant has to be different than zero: $\det(A) \neq 0$.

The first factorization method to be presented is the LU decomposition. If $\det(A) \neq 0$ there exists a decomposition such that:

$$A = LU \tag{3.8}$$

with L being lower triangular and U being upper triangular. The solution to the linear system is obtained in two steps, first let $y = Ux$, then:

$$Ly = b \tag{3.9}$$

where y is solved by forwards substitution using 3.4. The second step obtains x using:

$$Ux = y \tag{3.10}$$

and backwards substitution using 3.5.

Another factorization method widely used in state estimation is the Cholesky factorization. This method produces a decomposition of the matrix A of the form:

$$A = LL^T \tag{3.11}$$

Where L is lower triangular and L^T is its transpose. This decomposition exists if the matrix A is positive definite which means that $x^T Ax > 0$ for all vectors x . The solution x is obtained via two triangular systems, analogous to the LU factorization. Let $y = L^T x$, the first system to be solved is $Ly = b$ which gives the vector y . Then, $L^T x = y$ is solved to obtain the desired x vector. The Cholesky factorization is widely used in the WLS estimator because, for observable systems, the Gain matrix is symmetric and positive definite.

Additionally, there is the QR factorization. The definition of the QR factorization states that a matrix $A \in \mathfrak{R}^{m \times n}$, with $m \geq n$ admits a QR factorization if there exists an orthogonal matrix $Q \in \mathfrak{R}^{m \times m}$ and an upper trapezoidal matrix $R \in \mathfrak{R}^{m \times n}$ such that (QUARTERONI; SACCO; SALERI, 2000):

$$A = QR \tag{3.12}$$

Since this factorization can be applied in a rectangular matrix, R is trapezoidal and therefore has null rows from the $n + 1$ row up to m . The orthogonality property of the matrix Q means that $Q^T = Q^{-1}$, therefore a linear system $Ax = b$ can be solved with the following:

$$QRx = b \tag{3.13}$$

Multiplying both sides by Q^T and using the orthogonality property:

$$Q^T QRx = Q^T b \tag{3.14}$$

$$Q^{-1}QRx = Q^Tb \quad (3.15)$$

$$Rx = Q^Tb \quad (3.16)$$

Which is an upper triangular system that can be solved via backwards substitution using equation 3.5. Obtaining the QR factorization can be done by two main methods: Givens Rotations and Householder Reflections.

One important aspect of the QR factorization is the error analysis. In this topic, two concepts are important: forward and backwards stability. The first one is related to forward error which is a measure of how much the computed solution deviated from the real solution. Backwards stability is related to backwards error which is the error associated with the computed value given a small perturbation in the input data. The concept of backwards stability is specially important to DSSE because, as was shown, there can be a lot of factors that cause small perturbations on the input data leading to ill-conditioning. The QR factorization method is backwards and forwards stable as will be shown next.

The corresponding QR factorization satisfies:

$$\tilde{Q}\tilde{R} = A + \delta A \quad (3.17)$$

Where $\frac{\|\delta A\|}{\|A\|} = O(\epsilon_{machine})$. $\tilde{Q}\tilde{R}$ is the computed QR factorization of a slightly perturbed A , where the perturbation is represented as δA . The notation $O(\epsilon_{machine})$ represents an upper bound of this perturbation that is within the round-off error of floating point arithmetic ($\epsilon_{machine}$).

The forward step is stable (TREFETHEN; BAU, 1997) and proving the backwards stability means that:

$$(A + \Delta A)\tilde{x} = b \quad (3.18)$$

where $\frac{\|\Delta A\|}{\|A\|} = O(\epsilon_{machine})$. In other words, the computed solution \tilde{x} is exact even in the presence of an error in input data, represented by ΔA .

In order to prove the backwards stability of the QR factorization, it's necessary to show that the error ΔA is sufficiently small when the QR factorization is used to solve the linear system. The first step in the proof is to write $A + \Delta A$ as:

$$(\tilde{Q} + \delta Q)(\tilde{R} + \delta R)\tilde{x} = b \quad (3.19)$$

$$[\tilde{Q}\tilde{R} + \tilde{Q}(\delta R) + (\delta Q)\tilde{R} + (\delta Q)(\delta R)]\tilde{x} = b \quad (3.20)$$

Since $\tilde{Q}\tilde{R} = A + \delta A$, and δA is small when compared to A , we can write:

$$\frac{\|\tilde{R}\|}{\|A\|} \leq \|\tilde{Q}^T\| \frac{\|A + \delta A\|}{\|A\|} = O(1) \quad (3.21)$$

Using equation (3.21) and adding the terms of equation (3.20) we can show that:

$$\begin{aligned} \frac{\|\Delta A\|}{\|A\|} &\leq \frac{\|\delta A\|}{\|A\|} + \frac{\|(\delta Q)\tilde{R}\|}{\|A\|} + \\ &+ \frac{\|(\delta R)\tilde{Q}\|}{\|A\|} + \frac{\|(\delta Q)(\delta R)\|}{\|A\|} = O(\epsilon_{machine}) \end{aligned} \quad (3.22)$$

which concludes the proof of backwards stability.

Regarding the solution to the linear system $Ax = b$, one important consequence of the backwards stability of the QR algorithm is that the obtained solution \tilde{x} follows:

$$\frac{\|\tilde{x} - x\|}{\|x\|} = O(K(A)\epsilon_{machine}), \quad (3.23)$$

where $K(A)$ is the condition number of the matrix A and x is the exact solution of the system. Equation 3.23 shows that the error on the computed solution is a function of the condition number of the matrix A . In the context of the state estimator, this means that reducing the condition number of the coefficient matrix is an essential step to improve the accuracy of the solution. The proposed estimator in this work will accomplish this in later sections.

It was shown that small perturbations in the input data can have an effect on the computed solution and a backwards stable factorization method is important to reduce the backwards error, the next section will present ordering methods that reduce the creation of non-zero elements in the factorization process. These created elements can perturb the input data, increasing the ill-conditioning as well as increasing the memory necessity.

3.2.3 Ordering Methods

Usually, before the factorization process, the rows and columns of the matrix being factorized are reordered to reduce the number of fill-ins created. These fill-ins are elements originally zero that, because of the operations done by the factorization process, become non-zero. This problem is formulated as a optimization problem: obtain a permutation matrix P such as the factorization of $P^T A P$, where A is the matrix being factorized, produces the minimum amount of fill-in. (DAVIS, 2006; DAVIS; RAJAMANICKAM; SID-LAKHDAR, 2016). It has been shown by (YANNANAKIS, 1981) that this problem is NP-Complete and heuristics are used to solve it.

Some of these heuristics are based on the undirected graph associated with the matrix being factorized since a factorization step is equivalent to a node elimination. Fill-in is, therefore, new edges created in this graph after an elimination. This can be better visualized by Figure 3 where, after node 2 is eliminated, three new edges, in red, are created.

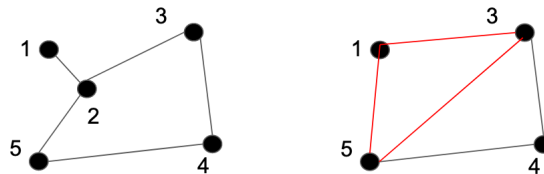


Figure 3 – Node elimination resulting in fill-ins. Source: Author

Choosing a different node to eliminate first in Figure 3 would result in another reduced graph, possibly with less fill-in. This is the basis of the heuristics which operate on the undirected graph, they produce an order of elimination that aims to minimize the fill-in created. The permutation which corresponds to this elimination order is then applied to the matrix so that the factorization steps occur in the same order as the elimination steps. What differs among heuristics is the criteria for choosing the next node to eliminate.

The MD (Minimum Degree) ordering produces a permutation matrix P that corresponds to the order obtained when the next node to be eliminated is the one with the minimum degree, that is, the one with the least amount of incident edges. In Figure 3, that node would be node 1 as a first choice to be eliminated. During the elimination process, it's possible that two or more nodes will have the same degree and some strategies to break these ties have been proposed in (GOMEZ; FRANQUELO, 1988). The first strategy selects among the nodes with the same minimum degree, the one with fewer adjacent nodes that have already been eliminated. Another strategy, called MD-ML (Minimum Degree, Minimum Length), builds a structure called path graph and selects among the tied nodes the one with minimum length or depth, as presented in (BETANCOURT, 1988). Since these first implementations of the minimum degree ordering, the method has improved a lot in terms of memory usage and performance but still maintains the basic idea of selecting the node with minimum degree as the next one in the elimination process. The Approximate Minimum Degree (AMD) ordering is the state-of-the-art method widely used in commercial packages and implementations and it is proposed in (AMESTOY; DAVIS; DUFF, 2004).

Another ordering method based on the graph of the matrix being factorized is called Nested Dissection. This method is iterative and uses the concept of divide and conquer to obtain a graph separator at each iteration that divides the original graph in

a manner that any path between the subgraphs passes through the separator. After a sufficient amount of iterations, any nodes not present in any separators are ordered first whereas the first separators are ordered last. Other heuristics can be used to order nodes in the subgraphs and separators that are not ordered by the Nested Dissection method.

Solving an ill-conditioned system requires a suitable method and, if possible, the use of sparse-oriented techniques such as ordering methods. The QR factorization is a backwards stable method, therefore, it is robust to small variations in the input data. The ordering methods presented result in a permutation matrix that, when applied to the coefficient matrix, result in less fill-in during the factorization process. The next section will present an algorithm that combines the backwards stable method with highly optimized sparse techniques. All of the previously mentioned reordering techniques can be used with the algorithm shown in the next section.

3.2.4 Multifrontal QR

Combining the concepts presented in the previous sections, this work presents a method that solves a linear system via QR factorization. The operations are optimized for sparse matrices and the previously shown fill-in reducing techniques can be used. This method is called Multifrontal QR. The major steps performed on this algorithm are shown in Figure 4.

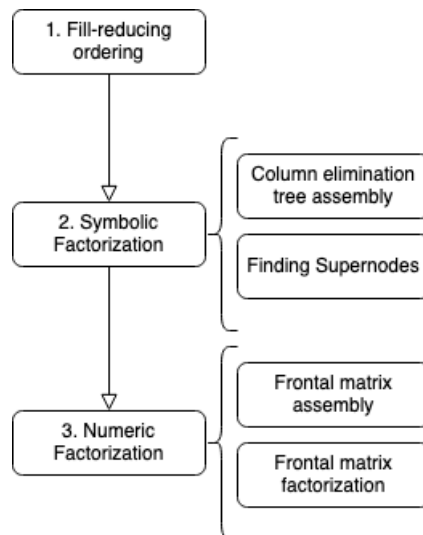


Figure 4 – Steps performed on the Multifrontal QR. Source: Author

The Multifrontal QR performs operations on groups of rows and columns of the matrix being factorized in order to work the majority of the computations in parallel. In contrast, traditional orthogonal methods are sequential, performing only on one row or column at a time which causes an irregular access of memory reducing computational performance (GEORGE; LIU; NG, 1988; GEORGE; HEATH, 1980). The Multifrontal

QR consists of three main steps, as shown in Figure 4, that result in the solution to the linear system. The first step is the reordering of the matrix in which a fill-in reducing permutation is obtained and then applied. The second step takes this reordered matrix and performs a symbolic analysis that results in the non-zero pattern of the resulting R factor. This analysis is used to guide and manage the operations that will be performed in the third phase which consists of the proper factorization and solving, via backwards substitution. This last step, the numeric factorization, is applied on so called Frontal Matrices which can be dense, that is, have a large number of non-zero elements.

Phase one of the Multifrontal QR, the reordering phase, consists mainly of applying one of the methods discussed in section 3. In summary, a permutation of the matrix being factorized is obtained which aims to reduce the number of fill-in required. Let A be the matrix being factorized, a permutation P is obtained so that the number of fill-ins in $P^T A P$ is minimized. For the sake of simplicity, the permutation matrix P is omitted from the notation.

The second phase called symbolic factorization assumes that the matrix has been reordered. In this second phase, a symbolic Cholesky factorization LL^T is applied without explicitly forming the matrix $A^T A$, instead, the structure of A is analyzed. The first step of this analysis is to obtain the elimination tree and compute the number of non-zero elements in each row of the factor R (GILBERT *et al.*, 2001). As is shown in Figure 4, the symbolic factorization step builds structures that will guide the numeric factorization.

The elimination tree has one node per column of R and can also be called column elimination tree. In order to build the tree, the nodes, which represent rows in the matrix, are connected to other nodes (called parent nodes) by applying the following rule: the parent node of i is k if k is the smallest row index greater than i where $r_{i,k} \neq 0$. After the elimination tree is built and the row pattern of the R factor is obtained, it is possible to group the nodes of the elimination tree that have the same pattern, here called supernodes. The group of nodes in a supernode represents a set of adjacent rows of the matrix A and this organization will later be used to form the so called frontal matrices in which the numeric step of the QR factorization will be applied. A secondary tree is built after finding the supernodes, this tree, called frontal matrix tree, has one node per supernode found which corresponds to one frontal matrix. In order to better visualize the method, Figure 5 shows a sparse matrix and its resulting factor R. The elimination tree is also presented and its supernodes are grouped together. As an example of the construction of this elimination tree, note that node 1 is a parent of node 2 because $r_{1,2} \neq 0$. Non-zero elements of the factor R are denoted by r in Figure 5. The resulting supernodes are grouped on the elimination tree by rectangles as well as the corresponding columns on the factor R in order to show the connection.

One important factor of the Multifrontal QR that improves its performance is

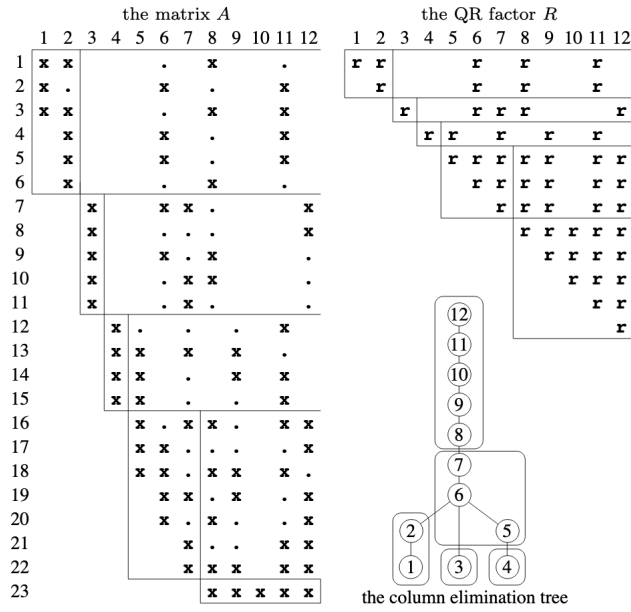


Figure 5 – A sparse matrix, its factor R and the elimination tree obtained with the Multifrontal QR. Source: (DAVIS, 2015)

the possibility of parallelism in its operations. The first possibility of parallelism arises from the frontal matrix tree assembly and factorization. In the example of Figure 5 the three frontal matrices that produce the first two rows of the matrix R can be assembled and factorized in parallel. The second possibility to take advantage of parallel routines is within each frontal matrix. The implementation of the Multifrontal QR used in this work is part of a state-of-the-art package named *SuiteSparse* that takes advantage of the aforementioned possibilities for parallelism.

3.3 Proposed Formulation

In the process of WLS state estimation for distribution system, several different factors can impact the solution as well as the iterative process, mainly the ill-conditioning associated with the Gain matrix. Other formulations were proposed to deal with this ill-conditioning but these alternatives formulations try to solve a modified problem, that is, a modified version of the state estimation process, that may not be entirely equivalent to the original problem (FENG; YANG; PETERSON, 2012). In this section, a orthogonal factorization is detailed and, because of this factorization, it is possible to obtain a state estimate via the WLS formulation without explicitly calculating the Gain matrix.

Using the notation from the Chapter 2, where the traditional formulation of the WLS estimator was presented, it is possible to apply an orthogonal factorization obtaining:

$$W^{1/2}H(x^k) = Q^T R \quad (3.24)$$

Rewriting the Normal Equation 2.9 as:

$$[R^T Q Q^T R] \Delta x^k = R^T Q W^{1/2} [z - h(x^k)] \quad (3.25)$$

Since $Q Q^T = I$, where I is the identity matrix, we obtain:

$$[R^T R] \Delta x^k = R^T Q W^{1/2} [z - h(x^k)] \quad (3.26)$$

Multiplying both sides by $(R^T)^{-1}$:

$$R \Delta x^k = Q W^{1/2} [z - h(x^k)] \quad (3.27)$$

From equation 3.27, it is possible to obtain the vector Δx^k using backwards substitution with the equation 3.5 since R was obtained via QR factorization and it is, therefore, upper triangular.

This formulation's main advantage in comparison with the WLS state estimator is the better conditioning. As was shown the condition number of a matrix directly impacts the quality and robustness of the solution of the linear system. Consider the condition number K of the upper triangular matrix R :

$$K(R) = \|R\| \|R^{-1}\| \quad (3.28)$$

Substituting from 3.24:

$$K(R) = \|[(Q^T)^{-1} W^{1/2} H]\| \|[(Q^T)^{-1} W^{1/2} H]^{-1}\| \quad (3.29)$$

Using the following property of inverse matrices:

$$(AB)^{-1} = B^{-1} A^{-1} \quad (3.30)$$

It is possible to rewrite $[(Q^T)^{-1} W^{1/2} H]^{-1}$, obtaining:

$$K(R) = \|[(Q^T)^{-1} W^{1/2} H]\| \|[(W^{1/2} H)^{-1} Q^T]\| \quad (3.31)$$

Approximating:

$$K(R) \approx \|(Q^T)^{-1}\| \|(W^{1/2} H)\| \|(W^{1/2} H)^{-1}\| \|Q^T\| \quad (3.32)$$

Since Q is orthogonal, the additional following properties are true: $Q^T = Q^{-1}$ and $\|Q\| = \|(Q^T)^{-1}\| = 1$, that is, the matrix Q is perfectly conditioned. Therefore we can approximate the condition number of R as:

$$K(R) \approx \|(W^{1/2} H)\| \|(W^{1/2} H)^{-1}\| = K(W^{1/2} H) \quad (3.33)$$

Equation (3.33) shows that the resulting system, when applying the proposed QR factorization to the WLS formulation, has a condition number of the same order of

magnitude as the Jacobian matrix whereas the system obtained with the Normal Equation has a condition number approximately the square of that of the Jacobian matrix.

The application of this orthogonal formulation can be associated with dedicated algorithms to take advantage of the sparse characteristics associated with the matrices of DSSE such as the Multifrontal QR which was presented in Section 3.2. The main structure of the State Estimator, however, remains very similar to that of the WLS state estimator. In summary: the network topology and measurement data are considered as inputs to the state estimator, calculations are performed to obtain the Jacobian matrix (in the case of the WLS state estimator, the Gain matrix is also calculated), the resulting linear system is then solved via QR factorization and the estimated state is updated until convergence is obtained. There are two main differences between the proposed orthogonal formulation and the WLS estimator: first, the Gain matrix does not need to be calculated and second, the QR factorization is used to solve the linear system instead of the commonly used Cholesky factorization. The aforementioned steps are better visualized in the diagram presented in Figure 6.

In order to use the orthogonal formulation, it is necessary to obtain the QR factorization of the matrix $W^{1/2}H$, which will be referred to as orthogonal QR matrix from now on. In Section 3.2, it was shown that the QR factorization is backwards stable, therefore, the advantages in terms of stability of this orthogonal formulation are twofold: the condition number of the orthogonal QR matrix is smaller than that of the Gain matrix and the process to obtain an estimated state makes use of a backwards stable factorization. This QR factorization can be obtained via Householder reflections or Givens rotations but, in order to extract peak computational performance, a dedicated algorithm is necessary. In this work, such algorithm was presented in Section 3.2 and this algorithm takes advantage of the sparse structures inherent to DSSE and uses state-of-the-art techniques to obtain the factorization in the least amount of time.

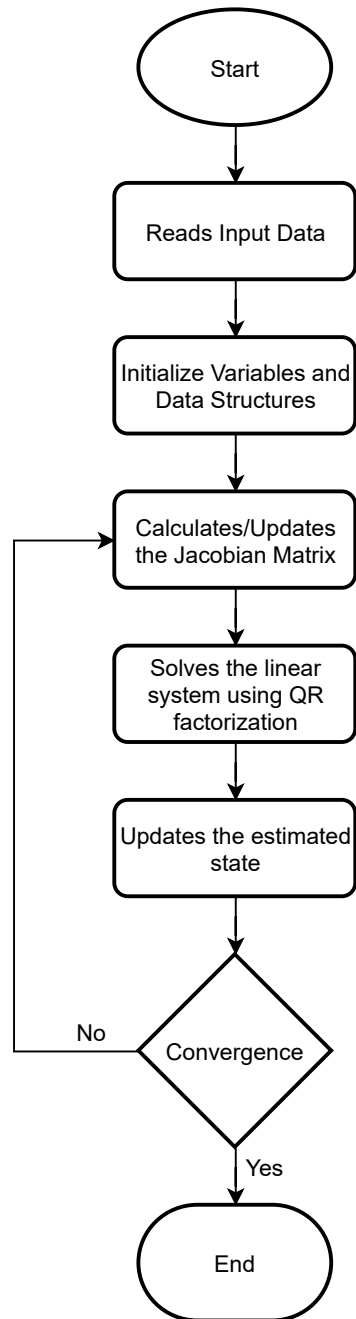


Figure 6 – Steps performed to obtain the estimated state with the orthogonal formulation of the state estimator.

4 RESULTS

4.1 Test Systems

In this chapter, the results obtained with the application of the sparse-oriented techniques mentioned in previous chapters will be presented. First, we present results with the application of fill-in reducing ordering with the intent to show what to expect in terms of memory improvement and computational efficiency. Since the application of these fill-in reducing ordering alone does not solve the central issue of DSSE, that is, the ill-conditioning of the Gain Matrix, it is necessary to apply a factorization method that can take advantage of the sparse structures. This method was presented in the previous chapter and because of the formulation presented that avoids the calculation of the Gain matrix, better-conditioned matrices are expected as well as improved performance while maintaining accuracy.

The simulations were performed in a machine that has a 2.7 Ghz core i5 with 8Gb of RAM on a Unix OS. All implementations were made with the C language. Three IEEE three-phase unbalanced test systems (SCHNEIDER *et al.*, 2017), widely used in the literature, were used to evaluate both the fill-in reducing ordering as well as the Multifrontal QR implementation. These systems have 34, 123 and 342 nodes and, along with a diverse set of measurements for each one, they represent different operating conditions and topology for distribution systems. In Table 2, the quantities of each measurement type contained in each test system is presented. The 34 nodes system has only SCADA measurements, whereas the 123 nodes system has a large number of virtual and pseudo-measurements with only a few SCADA measurements. The 342 nodes system has the greatest number of virtual measurements as well as smart meters, some SCADA measurements and no pseudo-measurements. All of these measurements are considered to be available at the same time, that is, different sampling rates are not in the scope of this work.

Table 2 – Measurements sets for the three different test systems

	34 nodes	123 nodes	342 nodes
SCADA measurements	632	72	575
Smart Meters	0	0	929
Pseudo-measurements	0	183	0
Virtual Measurements	0	316	1230

In terms of topology, the three systems have a very diverse set of characteristics. The 34 and 123 nodes systems are radial systems, that is, there is only one path from the substation to the terminal nodes or consumers. The first operates at a voltage level of 24.9 kV with a short 4.19 kV section. The second system has a nominal voltage of 4.16 kV. The

342 nodes system presents a complete scenario of operation since the low voltage network is modelled as well as the medium voltage network. The primary network operates at 13.2 kV. In Figure 7, the topology of the 342 nodes test system is presented where the medium voltage network is red and the low voltage network is blue, it is important to note that this system contains meshes which is unusual for distribution systems.

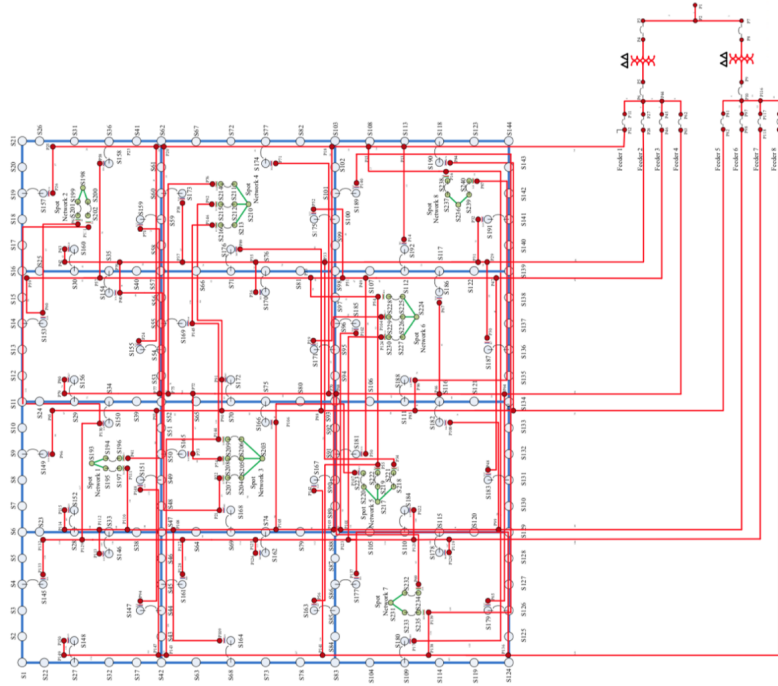


Figure 7 – Topology of the 342 nodes system

4.2 Evaluation of Ordering Methods

The fill-in reducing ordering methods presented in Chapter 3 were evaluated using the three test systems with the measurements sets shown in Table 2. The main goal of this simulation is to verify the improvement in data storage necessary and also computational performance in both the traditional formulation using the Gain matrix and also the proposed QR formulation. For the 342 nodes system without fill-in reducing ordering, the sparsity pattern of the Gain matrix as well as the $W^{1/2}H$ matrix obtained with the orthogonal QR method are shown in Figure 8. The sparse structure of the L factor obtained with the Cholesky factorization of the Gain matrix as well as the R factor obtained with the QR factorization of $W^{1/2}H$ are shown.

In Figure 8, it is also possible to see the influence of the topology of the system. Since the 342 nodes system has meshes, there are a high number of elements away from the diagonal. In contrast, Figure 9 presents the sparse structure of the Gain matrix as well as the $W^{1/2}H$ for the 123 nodes system and since this is a radial system, much fewer off-diagonal elements are present.

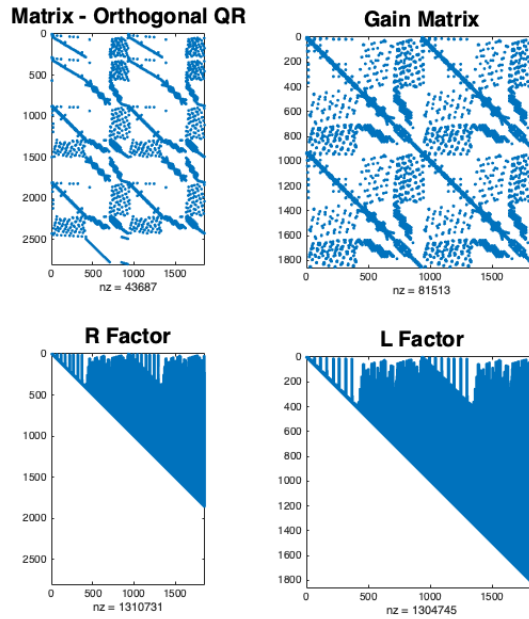


Figure 8 – Sparse pattern of the matrices of the 342 nodes IEEE test system and its corresponding factors

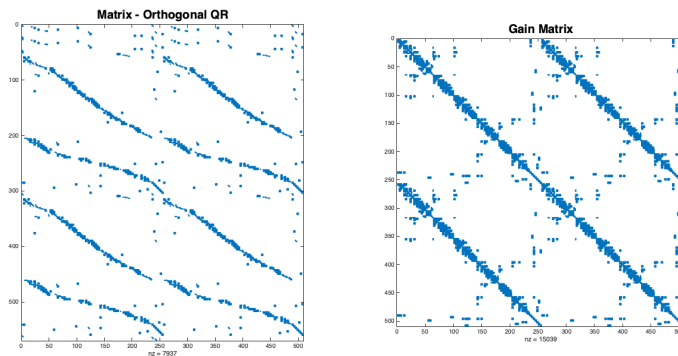


Figure 9 – Sparsity pattern of the matrices of the 123 nodes IEEE test system

The ordering methods presented in Chapter 3 were evaluated on the three test systems. AMD and Nested Dissection ordering methods were applied to both the Gain matrix and the $W^{1/2}H$ matrix of the orthogonal method presented in Chapter 3. It is important to note that, since the orthogonal matrix is not square, only its columns are reordered. In order to better illustrate the effect of this reordering, Figure 10 presents the sparsity structure of the 342 node system of the reordered Gain matrix and the L factor obtained with Cholesky factorization for the two ordering methods considered. At first glance, it is remarkable the reduction in fill-in when compared with the sparsity pattern when no ordering method is used, in Figure 8.

The reduction in fill-in is also expressive when considering the orthogonal QR formulation shown in Chapter 3. The sparsity pattern of the 342 nodes system of the matrix $W^{1/2}H$ and its factor R, from the QR factorization are shown in Figure 11. Since

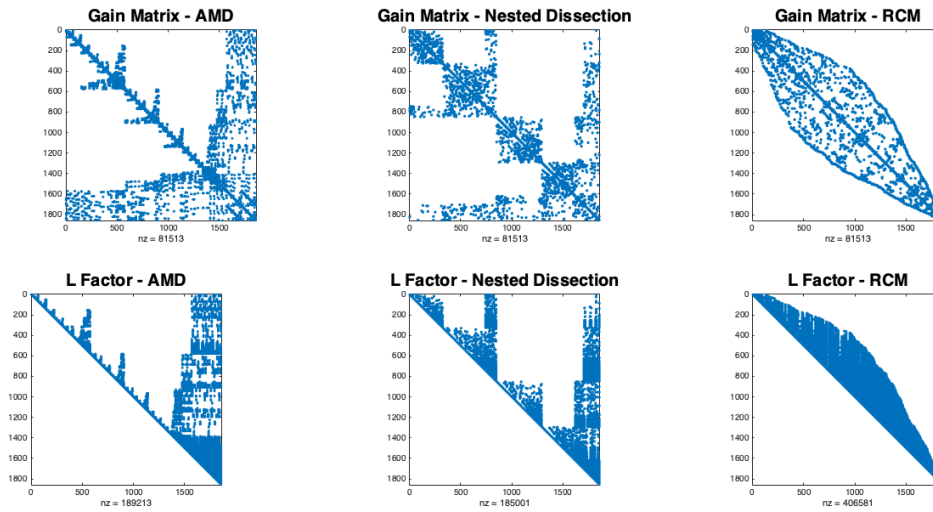


Figure 10 – Sparsity pattern of the ordered Gain matrix and its corresponding L factor, 342 nodes test system.

the ordering is only applied to the columns of the matrix, the sparse structure is not as organized as those observed in the ordered Gain matrix in Figure 10. Even though it is not possible to observe the effect of the ordering quite as clear with the matrix $W^{1/2}H$, the reduction of fill-in in the corresponding factor R is pretty extensive.

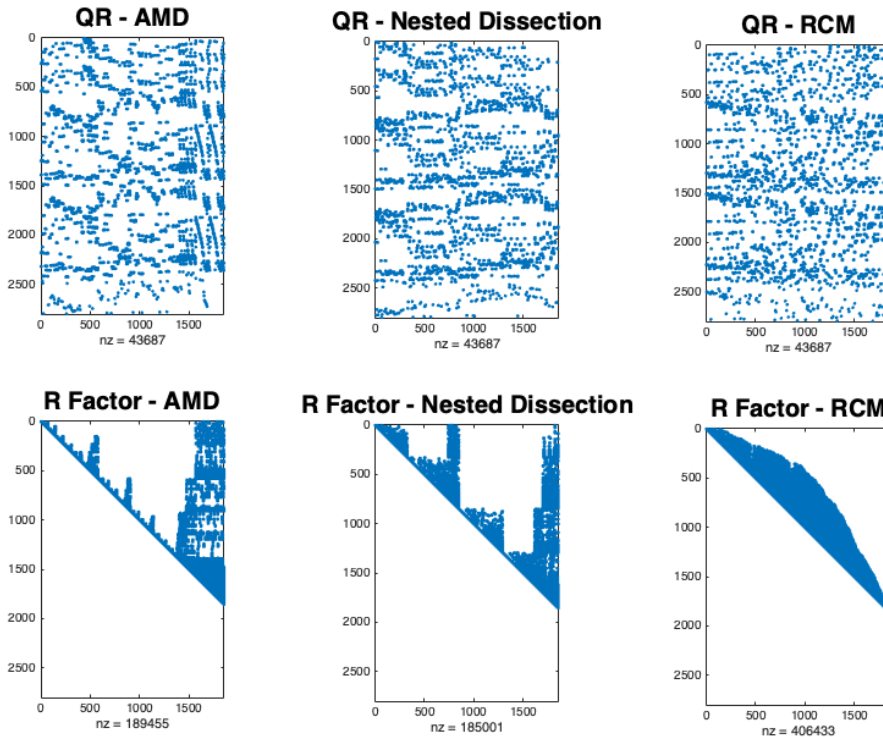


Figure 11 – Sparsity pattern of the ordered orthogonal QR matrix and its corresponding L factor, 342 nodes test system.

The results shown so far are from the 342 nodes system however, all systems were evaluated with the three ordering methods presented. The compiled results can be seen in Tables 3 and 4. The percentages represent the reduction of non-zero elements present in the Gain matrix, for Table 3, and in $W^{1/2}H$, for Table 4 compared to these matrices without a fill-in reducing ordering. Just as can be seen with the sparsity patterns, the numbers show a significant reduction in fill-in when ordering methods are applied. The minimum reduction obtained was 65,29% in the 34 nodes system when using Nested Dissection, specifically with the orthogonal QR formulation. For the 123 nodes system, fill-in was reduced by at least 88,96% and the largest system, with 342 nodes, showed a minimum reduction of 68,99%.

Table 3 – Relative fill-in reduction with the Gain Matrix formulation

	34 nodes	123 nodes	342 nodes
AMD	77,44%	90,97%	87,52%
Nested Dissection	71,73%	90,20%	87,80%
RCM	77,44%	90,97%	73,19%

Table 4 – Relative fill-in reduction with the proposed QR formulation

	34 nodes	123 nodes	342 nodes
AMD	72,30%	89,84%	85,55%
Nested Dissection	65,29%	88,96%	85,89%
RCM	71,29%	89,79%	68,99%

With the results shown so far, it becomes clear that using a fill-in reducing ordering is essential to improve performance both in terms of memory usage and also computational time. Memory usage is reduced because fewer elements need to be kept and the execution time is improved because fewer operations need to be performed. However, to obtain even more expressive gains in performance, the ordering methods need to be coupled with factorization methods that take advantage of sparse structures and optimizations. One of those methods was shown in Chapter 3, the Multifrontal QR is an algorithm specialized in dealing with large sparse matrices and because of that it uses the fill-in reducing ordering as one of the steps in the factorization process.

4.3 Evaluation of the Proposed QR Estimator

The following results were obtained in order to evaluate an implementation of the Multifrontal QR along the orthogonal factorization proposed in Chapter 3. Both the accuracy of this proposed formulation and the performance gains are metrics to evaluate the proposals and a methodology of tests was designed. This methodology, in summary, uses Monte Carlo simulations to create different measurement values from reference values

obtained with a power flow calculation. Each simulation results for a given Monte Carlo repetition, the estimated state values, are stored in order to evaluate the accuracy of the proposed algorithm using metrics such as the MAE (Mean Absolute Error):

$$MAE_i = \frac{1}{n_{trials}} \sum_{k=1}^{n_{trials}} |\hat{x}_i^k - x_i^{ref}|, \quad (4.1)$$

where \hat{x}_i is the i -th estimated variable x_i^{ref} is its corresponding reference value, k represents each repetition of n_{trials} simulations of the Monte Carlo method. Another useful metric evaluated is the Kema, based on (KEMA, 2006):

$$Kema^k = \frac{1}{n_{bus}} \sqrt{\sum_{j=1}^{n_{bus}} \sum_{\phi=1}^{n_{phases}} (|V_j^{\vec{\phi}} - V_j^{\vec{\phi},ref}|)} \quad (4.2)$$

where $V_j^{\vec{\phi}}$ is the complex voltage of phase ϕ at bus j and $V_j^{\vec{\phi},ref}$ is the reference voltage value of the same phase ϕ and at the same bus j . Also, k represents each repetition of n_{trials} simulations of the Monte Carlo method and n_{bus} is the total number of nodes in the system.

In more details, the test methodology consists of creating a measurement set that is different from that of the Table 2. A reference value for the measurements was generated from an exact load flow solution and random errors were included in each Monte Carlo simulation using the formula:

$$z_i = z_i^{lf} + u_i \cdot \sigma_{zi}, \quad (4.3)$$

where z_i is the value of the i -th measurement that will constitute the input data for a given simulation of the proposed algorithm, z_i^{lf} is the corresponding reference value for i -th measurement obtained from an exact load flow solution, u_i is a random variable that follows $u_i \sim N(0, 1)$, that is, zero mean and unitary standard deviation and finally σ_{zi} is the standard deviation of the i -th measurement given by:

$$\sigma_{zi} = \frac{|z_i^{lf}| pr_i}{3}, \quad (4.4)$$

where pr is the precision associated with each type of measurement. In this work, the following values were used: 30% for pseudo-measurements, 5% for smart-meter measurements, 2% for active and reactive power injection measurements, 1% for voltage magnitude measurements and 0.0001% for virtual measurements.

This methodology was specifically applied to the 342 nodes system and three different sets of measurements were created. The first one contains mostly pseudo-measurements and no smart-meter measurements. In the second one, a high number of smart-meter measurements were used and, in the third scenario, SCADA measurements of power flow in transformers were added to the measurement set of the second scenario. Simulations were

performed with 100 Monte Carlo repetitions for each measurement scenario previously presented. The condensed results, average MAE and KEMA metrics, are presented in Table 5, which also contains the condition number of the corresponding matrices $W^{1/2}H$ and G . As it is expected, the condition number of G is approximately the square of the condition number of $W^{1/2}H$.

Table 5 – Performance metrics obtained with the proposed estimator for each simulation scenario with the 342 nodes test system.

Scenario	MAE	Kema	$K(W^{1/2}H)$	$K(Gain)$
1	0.0005851	3.5981e-05	6.6843e+09	5.5326e+18
2	0.0004079	2.0207e-05	1.3536e+10	1.4447e+18
3	0.0004130	1.7887e-05	8.7496e+11	6.4480e+21

The MAE and Kema metrics were also graphed in order to visualize the simulation results for each Monte Carlo simulation and also for each state variable. In Figure 12, is presented the average value of the MAE metric for each state variable, this metric is also condensed on Table 6 where the average MAE is presented for each scenario as well as the Global Redundancy (GR) of the measurement set used. Also in Figure 12, the state variables in the high voltage (HV) system are highlighted as well as medium voltage (MV) and low voltage (LV). In Figure 13 the KEMA metric obtained in each Monte Carlo repetition is presented.

Table 6 – Detailed errors for all simulation scenarios obtained with the proposed estimator using the 342 nodes test system.

Scenario	Magnitude Error (p.u.)	Angle Error (p.u.)	GR
1	6.0290e-04	5.6715e-04	1.12
2	4.2891e-04	2.9507e-04	1.28
3	3.9800e-04	2.4537e-04	1.50

The proposed algorithm returned the worst performance when applied for Scenario 1, mainly because of the reduced number of measurements (the global redundancy (GR) of Scenario 1 is lower than the others).

4.4 Comparisons with Other Estimators

The results presented so far show that the proposed QR estimator, using the sparse oriented factorization and the Multifrontal QR algorithm is accurate in a diverse set operational conditions. It has been shown as well that the reordering techniques have a significant impact in fill-in created during the factorization which can impact computational performance. Since performance is one of the requirements for the state estimator in the

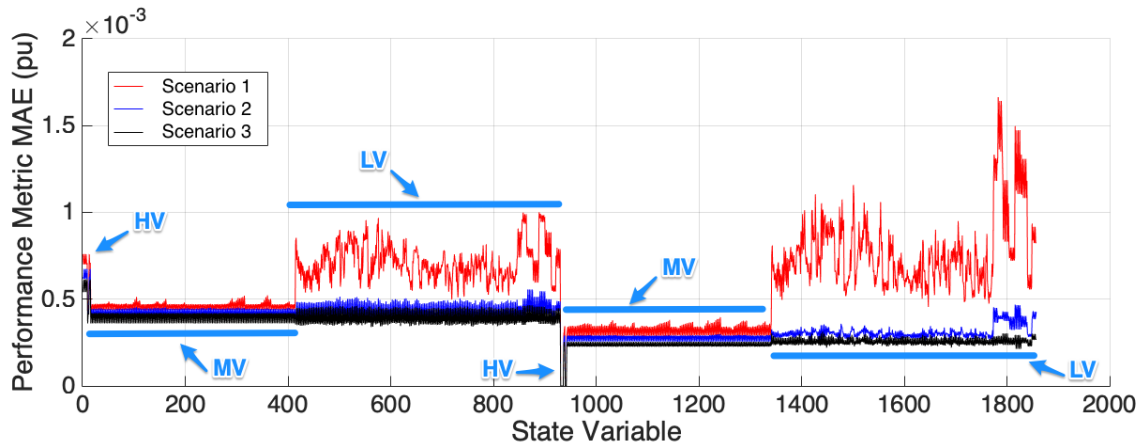


Figure 12 – Average MAE metric for all state variables

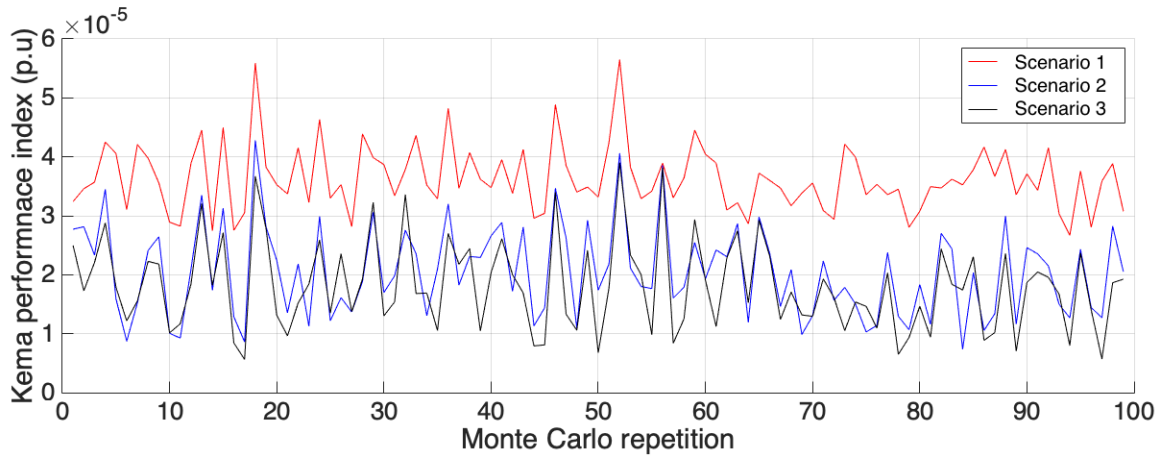


Figure 13 – KEMA metric for each Monte Carlo repetition

context of real-time operation of distribution system, simulations were carried to evaluate the computational aspects of the proposed QR estimator in comparison with the WLS state estimator with the Normal Equation (WLS-NE) and also the alternative formulations that were presented in previous chapters. These formulations are the WLS with Equality Constraints (NEC) and the Hatchel Augmented Matrix Method (Hatchel).

4.4.1 Numerical Aspects

The first result obtained was the condition number of the coefficient matrix in each of the estimators. In the case of the WLS-NE state estimator, this matrix is the Gain matrix. In the Proposed QR, this matrix is the $W^{1/2}H$ that is factorized to solve the corresponding linear system. For the NEC and Hatchel estimators, these matrices are the ones shown in equations 2.30 and 2.36, respectively.

Table 7 presented the results obtained for the three IEEE test systems used. At first glance it's possible to see the high condition numbers associated with the Gain matrix. The proposed QR estimator reduces the condition number as is expected since the Gain matrix is not built. The NEC estimator, however, did not reduce the condition number which shows that the higher weights associated with virtual measurements are not the only factor that impact the condition number. The Hatchel estimator greatly reduced the condition number, even more so than the Proposed QR for the smaller systems whereas for the 342 nodes system the numbers are pretty close.

Table 7 – Condition number of the coefficient matrix for different estimators.

System	WLS-NE	Proposed QR	NEC	Hatchel
IEEE34	3.4340e+18	1.0930e+10	1.0570e+26	2.3107e+06
IEEE123	1.7140e+17	1.0910e+09	2.4250e+18	6.1264e+05
IEEE342	1.6460e+21	8.7520e+11	8.4320e+23	7.3182e+10

Further simulations were performed on the NEC estimator since a scaling factor can be used to decrease the condition number of the matrix. Two options for factors were evaluated, the first one, α_1 , is:

$$\alpha_1 = \frac{1}{\max\{R_{ii}^{-1}\}} \quad (4.5)$$

And the second one, α_2 is:

$$\alpha_2 = \frac{m}{\sum_{i=1}^m R_{ii}^{-1}} \quad (4.6)$$

The results are shown in Table 8, the scaling factor α_1 performed better than α_2 on reducing the condition number of the coefficient matrix. It's noteworthy that the second factor increased the condition number of the matrix for the larger, 342 nodes, test system. Preliminary simulations showed that even though the condition number is improved, using a scaling factor impacts on the convergence of the estimator. Because of this, all future simulation will not be using any scaling factor.

Table 8 – Condition number of the coefficient matrix of the NEC estimator for different scaling factors.

System	α_1	α_2
IEEE34	1.009+17	2.060e+24
IEEE123	2.040e+14	6.800e+17
IEEE342	3.920e+17	1.160e+36

4.4.2 Computational Aspects

The first metric for computational performance that was evaluated was the number of iterations necessary for convergence, given a specified tolerance, of the estimators. In these simulations, in addition to the previously mentioned estimators, the Branch Current formulation was also included given that it is a dedicated estimator for distribution systems and it has been shown to be pretty fast. Tables 9, 10 and 11 presents the results in three different simulations: in the first one the coefficient matrix was not reordered, in the second one the AMD method was used to reduce fill-in and in the third one the Nested Dissection method was used to reorder the matrix. The Branch Current converged in the smallest number of iterations in the 34 and 123 nodes systems however it did not converge for the larger 342 nodes system. The main reason is the presence of meshes in this network. (BARAN, 2012) proposes a solution to weakly meshed networks in which an equality constraint is added to represent Kirchoff's law of currents in the loop. This addition could help convergence at the expense of performance.

Between the three results, with and without reordering, it's possible to see that the use of the both ordering methods greatly impacted the convergence of the NEC estimator. Without reordering, this estimator did not converge for the largest two systems whereas with the AMD method, it converged. When using the Nested Dissection method the NEC estimator converged for the two smaller systems. This result indicates that the fill-in impacts the factorization process and can lead to a non-convergence.

Table 9 – Number of iterations necessary for convergence for each estimator without reordering the coefficient matrix.

System	WLS-NE	Proposed QR	NEC	Hatchel	Branch Current
IEEE34	NC	5	NC	5	3
IEEE123	NC	4	NC	4	3
IEEE342	NC	4	NC	4	NC

Table 10 – Number of iterations necessary for convergence for each estimator using the AMD ordering method.

System	WLS-NE	Proposed QR	NEC	Hatchel	Branch Current
IEEE34	NC	5	6	5	3
IEEE123	NC	4	9	4	3
IEEE342	NC	4	8	4	NC

The second performance metric evaluated was the time necessary for convergence. Tables 12, 13 as well as 14 show the results without ordering of the coefficient matrix and with the AMD and with the Nested Dissection methods applied. Although the number

Table 11 – Number of iterations necessary for convergence for each estimator using the Nested Dissection ordering method.

System	WLS-NE	Proposed QR	NEC	Hatchel	Branch Current
IEEE34	NC	5	4	5	3
IEEE123	NC	4	3	4	3
IEEE342	NC	4	NC	4	NC

of iterations did not change for the Proposed QR and Hatchel methods between these scenarios, the estimation time changed significantly between the ordered and non ordered simulations. For the 342 nodes system, for example, the Hatchel estimator needed 11.3 seconds for convergence without ordering and approximately 1.5 seconds when either method of ordering was applied. Between the AMD and Nested Dissection method there is a small difference in execution times but neither is significantly faster than the other.

The expressive difference in times obtained with and without ordering shows the impact of the fill-in reduction in computational performance of these estimators. The Branch Current estimator, on the other hand, does not improve with the ordering possibly because its coefficient matrix is constant and linear. Overall, as was expected, the Branch Current estimator was the fastest among the two smallest systems. For the 342 nodes test system, with the AMD reordering, the Proposed QR obtained the smallest estimation time.

Table 12 – Time necessary for convergence for each estimator without reordering the coefficient matrix.

System	WLS-NE	Proposed QR	NEC	Hatchel	Branch Current
IEEE34	NC	0.1180	NC	0.07713	0.006769
IEEE123	NC	0.2131	NC	0.2939	0.02374
IEEE342	NC	2.5949	NC	11.3795	NC

Table 13 – Time necessary for convergence for each estimator using the AMD ordering method.

System	WLS-NE	Proposed QR	NEC	Hatchel	Branch Current
IEEE34	NC	0.09730	0.1013	0.06324	0.006065
IEEE123	NC	0.1721	0.1269	0.1368	0.01891
IEEE342	NC	1.1994	3.5580	1.5488	NC

The previous comparisons were performed to evaluate computational aspects of different state estimators that may be applied to distribution systems. Previously in the chapter, results were also presented that show the accuracy of the Proposed QR in three simulation scenarios as shown in Table 5. The next results extend these simulations using,

Table 14 – Time necessary for convergence for each estimator using the Nested Dissection ordering method.

System	WLS-NE	Proposed QR	NEC	Hatchel	Branch Current
IEEE34	NC	0.1065	0.05183	0.05638	0.006842
IEEE123	NC	0.1886	0.2073	0.1381	0.02016
IEEE342	NC	1.2207	NC	1.4417	NC

for the 342 nodes test system, the measurement scenario 1 and 100 Monte Carlo repetitions for each test system. The condensed results are presented in Table 15 where for each estimator, the maximum MAE value obtained is shown. The NEC estimator did not converge for some of the measurement sets created during the Monte Carlo repetitions and therefore, no MAE value could be calculated. This shows that this formulation may be highly sensitive to variations in the input data. The most accurate estimation, according to Table 15, is the Proposed QR formulation closely followed by the Hatchel formulation. The Branch Current formulation, on the other hand, has shown the highest MAE value although it showed the fastest times on Tables 12, 13 and 14.

Table 15 – Maximum MAE considering all Monte Carlo simulations.

System	WLS-NE	Proposed QR	NEC	Hatchel	Branch Current
IEEE34	NC	0.006590	0.08828	0.01201	0.08603
IEEE123	NC	0.003703	NC	0.003436	0.03850
IEEE342	NC	0.001293	NC	0.002114	NC

5 CONCLUSIONS

The state estimator is the main tool for real-time analysis of power systems. Given the recent increase in smart meters usage, distributed generation and even electric vehicles, the utilities now face a new challenge to obtain the operating condition of distribution systems. Historically, the absence of measurements was a hindrance to DSSE and the operating condition of the network was obtained with load profiles which can vary substantially from feeder to feeder. The WLS estimator, commonly used in transmission systems, faces difficulties in distribution systems caused mainly by the ill-conditioning associated with the Gain matrix. The causes of this ill-condition were detailed in chapter 3 and alternative formulations have been proposed. In chapter 3, an orthogonal factorization was proposed that uses the WLS formulation but avoids calculating the Gain matrix and, as presented in chapter 4, greatly improves computation performance while maintaining accuracy. The improvement in computational performance, however, cannot only be attributed to the orthogonal method presented in chapter 3. The use of ordering methods to preserve the sparse nature of the matrices as well as a factorization algorithm specialized in sparse structures also greatly improves performance.

The results show that taking advantage of the sparse nature of the matrices associated with the WLS state estimator in distribution systems can be beneficial to improving computational efficiency without losing accuracy. If a robust factorization method is coupled with a reordering step, using for example the AMD or METIS method, fill-in is greatly reduced which in turn decreases computational effort and increases performance. Another important aspect of this work is the use of detailed two-port model for the network equipment which better represents their electrical characteristics while also being flexible enough to be used with a diverse set of networks configurations and infrastructure.

Simulations were performed comparing the WLS state estimator with the Normal Equation and its variations such as the WLS with Equality Constraint (NEC) and Hatchel Augmented Matrix Method with the Proposed QR method. A well established dedicated estimator for distribution systems was also simulated, the Branch Current state estimator. The results obtained showed that it is the fastest among all estimator considered but, because of its simplifications in the measurement set, it obtained the lowest accuracy among all simulations.

The conclusion of this work is that, given the ill-conditioning of the WLS-NE, it is not a suitable choice for distribution systems. An alternative formulation, either the NEC or Hatchel, is necessary in order to obtain convergence for the IEEE test systems considered and the use of a reordering method greatly improves computational

time. Further performance gains can be achieved with the use of the dedicated Branch Current Estimator however these gains come at the expense of accuracy. The Proposed QR estimator presented in chapter 3 is a great balance between speed and accuracy: it obtained adequate times for all test systems while showing good accuracy.

5.1 Future Research

Given what was presented in this work, there are a few possibilities for future research: since the two-port model is quite flexible, other network configurations and types of equipment could be studied such as DC links in the distribution network. Further research is necessary to understand how these links would impact the two-port model and how the simulation would perform. Another benefit of the three-phase model flexibility is the possibility to extend the application of the Proposed QR estimator to a more complete system, including transmission and sub-transmission systems. How it was presented, the algorithm is numerically robust and performs quite well when applied to large distribution systems and future research with more complete systems may show that it can also be applied with satisfactory results.

Other measurement models could be studied. For example, there are extensions of the estimators presented that include PMU (Phasor Measurement Units) measurements with different sampling rates than those of SCADA measurements. When used with the dedicated Branch Current Estimator, these measurements have been shown to increase accuracy. On the other hand, the proposals to include PMU measurements in the WLS estimator enter the domain of Dynamic State Estimation which is not the author's main area of study. It would be interesting to see if any of the techniques presented here could be used with these dynamic estimators.

5.2 List of Publications

The author has submitted some papers that present direct results of the research developed in this work. The main published work consists of the partial results presented in Chapter 5 as well as the orthogonal formulation presented in Chapter 4. The paper was presented in an international conference and published in a special edition of Electric Power Systems Research:

- HEBLING, G. M., MASSIGNAN, J. A. D., LONDON JR. J. B. A., CAMILLO, M. H. M. "**Sparse and numerically stable implementation of a distribution system state estimation based on Multifrontal QR factorization**". Electric Power Systems Research, 2020.

The ordering methods presented in Chapter 3 as well as the results obtained with

their application in different test systems were also submitted to a national conference. The following paper was published and presented at the conference:

- HEBLING, G. M., MASSIGNAN, J. A. D., LONDON JR. J. B. A., DANTAS, L. B. "**Análise de padrões de esparsidade e métodos de ordenação para estimação de estado em sistemas de distribuição**". Congresso Brasileiro de Automática - CBA, 2020.

As an extension of the work presented here, the author has published a paper using the orthogonal framework to detect bad data. The following paper was presented in an international conference showing that using an orthogonal formulation is also effective when detecting bad data as well as being quite fast.

- HEBLING, G. M., MASSIGNAN, J. A. D., LONDON JR. J. B. A., RENATO, R. "**Sparse and Orthogonal Method for Fast Bad Data Processing in Distribution System State Estimation**". IEEE Madrid PowerTech, 2021.

In parallel with the research presented in this work, the author has submitted a paper applying network equivalents to meshed distribution systems. The following paper has been accepted:

- HEBLING, G. M., MASSIGNAN, J. A. D., CAMILLO, M. H. M., LONDON JR. J. B. A. "**Aplicação de Equivalentes de Rede em Sistemas de Distribuição com Malha entre Subestações**". Simpósio Brasileiro de Sistemas Elétricos (SBSE), 2020.

REFERENCES

- ABUR, A.; EXPÓSITO, A. G. **Power System State Estimation: Theory and Implementation**. [*S.l.: s.n.*]: Nova York: CRC Press, 2004.
- AHMAD, F. *et al.* Distribution system state estimation-a step towards smart grid. **Renewable and Sustainable Energy Reviews**, 2018.
- AHMAD, F. *et al.* Distribution system state estimation-a step towards smart grid. **Renewable and Sustainable Energy Reviews**, 2018.
- ALMEIDA, M. C.; OCHOA, L. F. An improved three-phase amb distribution system state estimator. **IEEE Trans. Power Systems**, v. 32, n. 2, mar. 2017.
- ALMEIDA, M. C.; SCHINCARIOL, R.; OCHOA, L. F. Assessing the statistical consistency of the amb state estimator in distribution systems. **IEEE PES Innovative Smart Grid Technologies Latin America**, 2015.
- AMESTOY, P. R.; DAVIS, T. A.; DUFF, I. S. Algorithm 837: Amd,an approximate minimum degree ordering algorithm. **ACM Trans. Math.Softw**, 2004.
- ARRILLAGA, J.; HARKER, B. J. Fast-decoupled three-phase load flow. **Proceedings of the Institution of Electrical Enginners**, v. 125, n. 8, p. 734–740, August 1978.
- ATANACKOVIC, D.; DABIC, V. Deployment of real-time state estimatorand load flow in bc hydro dms - challenges and opportunities. **IEEE PES General Meeting, Vancouver BC**, 2013.
- BARAN, M. Branch current based state estimation for distribution system monitoring. **IEEE Power and Energy Society General Meeting**, 2012.
- BARAN, M.; MCDERMOTT, T. E. State estimation for real time monitoring of distribution feeders. **IEEE Power & Energy Society General Meeting**, 2009.
- BETANCOURT, R. An efficient heuristic ordering algorithm for partial matrix refactorization. **IEEE Transactions on power systems**, 1988.
- DAVIS, T. A. **Direct methods for sparse linear systems**. Philadelphia, PA: SIAM, 2006.
- DAVIS, T. A. Algorithm 915, suitesparse qr: multifrontal multithreaded rank revealing sparse qr factorization. **ACM Transactions on Mathematical Software**, 2015.
- DAVIS, T. A.; RAJAMANICKAM, S.; SID-LAKHDAR, W. M. A survey of direct methods for sparse linear systems. **Acta Numerica**, n. 25, p. 386–566, 2016.
- FENG, X.; YANG, F.; PETERSON, W. A practical multi-phase distribution state estimation solution incorporating smart meter and sensor data. **IEEE Power and Energy Society General Meeting**, 2012.
- GEORGE, A.; HEATH, M. T. Solution of sparse linear least squaresproblems using givens rotations. **Linear Algebra Appl**, 1980.

- GEORGE, A.; LIU, J. H. W.; NG, E. G. A data structure for sparseqr and lu factorizations. **SIAM J. Sci. Statist. Comput**, 1988.
- GILBERT, J. R. *et al.* Computing row and column counts for sparse qr and lu factorization. **BIT Numerical Mathematics**, 2001.
- GJELSVIK, A.; AAM, S.; HOLTEN, L. Hachtel's augmented matrix method - a rapid method improving numerical stability in power system static state estimation. **IEEE Transactions on Power Apparatus and Systems**, 1985.
- GOMEZ, A.; FRANQUELO, L. G. An efficient ordering algorithm to improve sparse vector methods. **IEEE Transactions on power systems**, 1988.
- HEBLING, G. M. *et al.* Sparse and numerically stable implementation of a distribution system state estimation based on multifrontal qr factorization. **Electric Power Systems Research (EPSR)**, 2020.
- KANJUH, G. V. S. S. Real-life distribution state estimation integrated in the distribution management system. **International Transactions on Electrical Energy Systems**, 2016.
- KEMA. Metrics for determining the impact of phasor measurements on power system state estimation,. **DRAFT**, January 2006.
- KERSTING, W. H. **Distribution system modelling and analysis**. Boca Raton, Florida: CRC Press, 2001.
- LEFEBVRE, S.; PRÉVOST, J.; LENOIR, L. Distribution state estimation: A necessary requirement for the smart grid. **IEEE PES General Meeting | Conference & Exposition**, 2014.
- LIN, W.; TENG, J. State estimation for distribution systems with zero- injection constraints. **IEEE Transactions on Power Systems**, v. 11, n. 1, 1996.
- LOURENÇO E. M.; LONDON JR., J. B. A. **Power Distribution System State Estimation**. [*S.l.: s.n.*]: UK, IET Publisher, 2022. ISBN 978-1-83953-201-6.
- MASSIGNAN, J. A. D. *et al.* In-field validation of a real-time monitoring tool for distribution feeders. **IEEE Trans. Power Delivery**, 2018.
- MONTICELLI, A.; MURARI, C. A. F.; WU, F. F. A hybrid state estimator:solving normal equations by orthogonal transformations,. **IEEE Trans.Power Appar. Syst.**, PAS-104, n. 12, p. 3460–3468, 1985.
- PAU, M.; PEGORARO, P. A.; SULIS, S. Efficient branch-current-based distribution system state estimation including synchronized measurements. **IEEE Transactions on Instrumentation and Measurement**, 2013.
- PAU, M.; PEGORARO, P. A.; SULIS, S. Wls distribution system state estimator based on voltages or branch-currents: Accuracy and performance comparison. **IEEE International Instrumentation and Measurement Technology Conference (I2MTC)**, 2013.
- PRIMADIANTO, A.; LU, C. A review on distribution system state estimation. **IEEE Trans. on Power Systems**, v. 32, n. 5, set. 2017.

-
- QUARTERONI, A.; SACCO, R.; SALERI, F. **Numerical Mathematics**. [*S.l.: s.n.*]: Springer, 2000.
- SCHNEIDER, K. P. *et al.* Analytic considerations and design basis for the ieeec distribution test feeders. **IEEE Transactions on Power Systems**, 2017.
- SIMOES-COSTA, A.; QUINTANA, V. H. An orthogonal row processing algorithm for power system sequential state estimation. **IEEE Trans. Power Appar. Syst.**, PAS-100, n. 8, p. 3791–3800, 1981.
- SIMOES-COSTA, A.; QUINTANA, V. H. A robust numerical technique for power system state estimation. **IEEE Trans. Power Appar. Syst.**, PAS-100, n. 2, p. 691–698, 1981.
- SINGH, R.; PAL, B.; JABR, R. Choice of estimator for distribution system state estimation. **IET Generation, Transmission & Distribution**, v. 3, n. 7, 2009. ISSN 17518687.
- THORNLEY, V.; JENKINS, N.; WHITE, S. State estimation applied to active distribution networks with minimal measurements. **Comput. Conf.**, n. 5, 2005.
- TREFETHEN, L. N.; BAU, D. **Numerical Linear Algebra**. [*S.l.: s.n.*]: SIAM, 1997.
- YANNANAKIS, M. Computing the minimum fill-in is np-complete. **SIAM Journal on Discrete Mathematics**, p. 77–79, 1981.